

Optimal Transportation and Alignment Between Gaussian Measures

Sanjit Dandapanthula^{†*} Aleksandr Podkopaev[‡] Shiva Prasad Kasiviswanathan[‡]
sanjitd@cmu.edu sashapod@amazon.com kasivisw@gmail.com

Aaditya Ramdas^{†§} Ziv Goldfeld^{||}
aramdas@cmu.edu goldfeld@cornell.edu

December 4, 2025

Abstract

Optimal transport (OT) and Gromov–Wasserstein (GW) alignment provide interpretable geometric frameworks for comparing, transforming, and aggregating heterogeneous datasets—tasks ubiquitous in data science and machine learning. Because these frameworks are computationally expensive, large-scale applications often rely on closed-form solutions for Gaussian distributions under quadratic cost. This work provides a comprehensive treatment of Gaussian, quadratic cost OT and inner product GW (IGW) alignment, closing several gaps in the literature to broaden applicability. First, we treat the open problem of IGW alignment between uncentered Gaussians on separable Hilbert spaces by giving a closed-form expression up to a quadratic optimization over unitary operators, for which we derive tight analytic upper and lower bounds. If at least one Gaussian measure is centered, the solution reduces to a fully closed-form expression, which we further extend to an analytic solution for the IGW barycenter between centered Gaussians. We also present a reduction of Gaussian multimarginal OT with pairwise quadratic costs to a tractable optimization problem and provide an efficient algorithm to solve it using a rank-deficiency constraint. To demonstrate utility, we apply our results to knowledge distillation and heterogeneous clustering on synthetic and real-world datasets.

[†]Carnegie Mellon University, Department of Statistics

[‡]Amazon Web Services (AWS) LogAnalytics

[§]Carnegie Mellon University, Machine Learning Department

^{||}Cornell University, Department of Electrical and Computer Engineering

*A large part of this work was done while SD was an intern at Amazon Web Services during Summer 2025.

1	Introduction	3
1.1	Contributions	5
1.2	Related Work	6
1.3	Notation	8
2	Background	9
3	IGW Alignment Between Gaussian Measures	11
3.1	IGW Distance and Optimal Coupling	12
3.2	IGW Barycenter Between Centered Gaussians	15
4	Multimarginal Problems Between Gaussian Measures	18
4.1	Multimarginal IGW	19
4.2	Multimarginal Optimal Transport	19
4.3	An Efficient Burer-Monteiro Algorithm for Multimarginal OT	21
5	Experiments	23
5.1	IGW Metric for Representation Similarity of Language Models	23
5.1.1	Existing and Proposed Similarity Metrics	23
5.1.2	Gaussian Modeling Assumption and Verification	24
5.1.3	LLM Representation Comparison via IGW	25
5.2	Heterogeneous User Clustering	26
5.3	Efficient Computation of Multimarginal OT	29
6	Conclusion	30
A	Proofs of Main Results	36
A.1	Proof of Theorem 3.1	36
A.2	Proof of Theorem 3.2	40
A.3	Proof of Corollary 3.1	41
A.4	Proof of Corollary 3.2	41
A.5	Proof of Theorem 4.1	42
A.6	Proof of Theorem 4.2	43
B	Recovering the Barycenter from Multimarginal IGW	44

C Optimal Transport Between Gaussian Measures	46
D Background on the OT and GW Problems	49
D.1 Optimal Transport	49
D.2 Gromov-Wasserstein Distances	51
E Background on Riemannian Optimization	54
F Background on Random Variables in Hilbert Spaces	55

1 Introduction

Comparing and aggregating heterogeneous datasets are fundamental aspects of modern data science and machine learning. To capture the geometry of the data corpus, it is standard to model datasets as probability distributions over high-dimensional manifolds. With this abstraction, two powerful frameworks for comparing probability distributions on the same or possibly different spaces, respectively, are *optimal transport (OT)* and *Gromov-Wasserstein (GW) alignment*; we depict the OT and GW problems in [Figure 1](#). The theory of OT gives rise to the Wasserstein distances, which in recent years have had a significant impact on the fields of statistics and machine learning, including for generative modeling ([Arjovsky et al., 2017](#); [Dukler et al., 2019](#); [Kwon et al., 2022](#); [Haviv et al., 2024](#)), domain adaptation ([Courty et al., 2017](#); [Lee et al., 2019](#)), and general data science ([Ho et al., 2017](#); [Mi et al., 2018](#); [Naumann et al., 2025](#)). In a similar vein, GW distances have found numerous applications in language modeling ([Alvarez-Melis and Jaakkola, 2018](#); [Kawakita et al., 2024](#)), single-cell genomics ([Demetci et al., 2022](#); [Klein et al., 2024](#)), computational geometry ([Koehl et al., 2023](#); [Chambers and Meng, 2025](#)), generative modeling ([Bunne et al., 2019](#); [Klein et al., 2023](#)), and graph matching ([Xu et al., 2019](#); [Brogat-Motte et al., 2022](#)).

Despite their utility, computation under the OT and GW frameworks is notoriously difficult. The Wasserstein distance between empirical distributions over n data points can be expressed as a linear program which can only be solved in $O(n^3 \log(n))$ time using interior-point methods or min-cost flow algorithms ([Peyré and Cuturi, 2019](#)). Even worse, computation of GW distances in the same setting requires solving a quadratic assignment problem, which is generally NP-hard ([Loiola et al., 2007](#)). Although there is recent work using entropic regularization ([Cuturi, 2013](#); [Rioux et al., 2024](#); [Zhang et al., 2024](#)), slicing ([Rabin et al., 2011](#); [Kolouri et al., 2019](#); [Nietert et al., 2022](#)), and neural estimation ([Makkuva et al., 2020](#); [Daniels et al., 2021](#); [Mokrov et al., 2024](#);

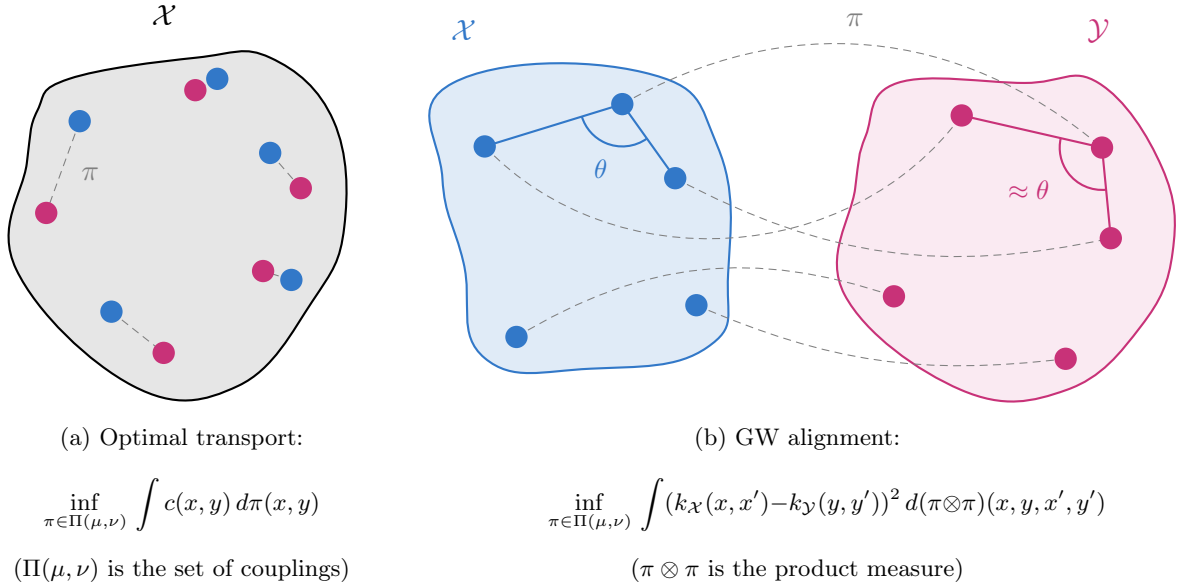


Figure 1: (a) The OT problem compares measures over the same space by searching for the coupling π which minimizes expected transportation cost $c(x, y)$. Here we depict the quadratic-cost OT problem, with $c(x, y) = \|x - y\|_2^2$. (b) GW alignment compares measures over (possibly different) spaces by searching for the coupling π which matches the kernels $k_{\mathcal{X}}$ and $k_{\mathcal{Y}}$ as well as possible. Here, we depict the inner product Gromov-Wasserstein (IGW) problem with $k_{\mathcal{X}}(\cdot, \cdot) = k_{\mathcal{Y}}(\cdot, \cdot) = \langle \cdot, \cdot \rangle$, which seeks to find a coupling which is as close to unitary as possible (roughly, preserving pairwise angles).

Wang and Goldfeld, 2024) for more efficient computation, explicit solutions which can be obtained in special cases of the OT and GW problems are of intense theoretical and practical interest. As an important example, the *Bures–Wasserstein* formulae for the 2-Wasserstein distance and barycenter between Gaussians have been heavily applied in the literature, including to linear metric learning (Cooper, 2023), knowledge distillation in machine learning (Lv et al., 2024), style transfer for image generation (Mroueh, 2019), and covariance estimation (Han et al., 2023).

Beyond these two landmark results and recent attempts to extend them to the GW setting (Le et al., 2022; Salmona et al., 2022), structured solutions under Gaussian distributions and quadratic-like costs are scarce. Motivated by the success of the Bures–Wasserstein formulae, this work studies explicit solutions for a breadth of OT and IGW problems between Gaussian measures, spanning the bimarginal, multimarginal, and barycentric settings, filling several important gaps in the literature.

1.1 Contributions

We first consider the bimarginal IGW distance between Gaussian measures on a general Hilbert space, for which only partial results are available; namely, [Salmona et al. \(2022\)](#) provide an expression restricted to centered Gaussians in \mathbb{R}^d , which is limiting since IGW is not translation invariant. We first present a reduction of the Gaussian IGW distance to a quadratic optimization problem over unitary operators. We then prove that the optimum is attained and provide the IGW optimal coupling in closed-form, up to the resolution of the aforementioned optimization problem. From the proof, we also deduce that the IGW distance between any two measures can be upper bounded by the Gaussian IGW with matched first and second moments, further motivating the Gaussianity assumption. We then prove tight upper and lower bounds on the squared IGW distance between uncentered Gaussian measures $\mu_1 = \mathcal{N}(m_1, \Sigma_1)$ and $\mu_2 = \mathcal{N}(m_2, \Sigma_2)$ of the form

$$\xi(\mu_1, \mu_2) - \|\eta(\mu_1)\| \|\eta(\mu_2)\| \leq \text{IGW}(\mu_1, \mu_2)^2 \leq \xi(\mu_1, \mu_2) - \langle \eta(\mu_1), \eta(\mu_2) \rangle,$$

where $\xi(\mu_1, \mu_2)$, $\eta(\mu_1)$, and $\eta(\mu_2)$ are analytically computable quantities in terms of m_1 , Σ_1 , m_2 , and Σ_2 . Noting that our upper and lower bounds coincide if $\eta(\mu_1)$ and $\eta(\mu_2)$ are aligned (by Cauchy-Schwarz), we obtain analytic solutions for the IGW distance between Gaussians under an alignment condition, which relaxes the centering assumption of [Salmona et al. \(2022\)](#). Since the only unitary operators on \mathbb{R} are ± 1 , we also analytically resolve the IGW distance between univariate Gaussians. Building on the bimarginal results, we generalize known formulae for the IGW barycenter between centered Gaussian measures ([Le et al., 2022](#); [Salmona et al., 2022](#)) to the Hilbert space setting and to the case of infinitely many measures.

Next, we treat the multimarginal OT ([Gangbo and Świąch, 1998](#)) and multimarginal IGW problems between Gaussians. Observing that the pairwise optimal bimarginal couplings can be glued together into a multimarginal coupling, we resolve the multimarginal IGW problem between centered Gaussians over separable Hilbert spaces in closed-form. Using similar techniques, we formulate the multimarginal OT problem between Gaussians as the solution of a semidefinite program and show that the solution must have low rank. When considering p Gaussian measures over \mathbb{R}^d , the rank-deficiency constraint together with the Burer-Monteiro factorization ([Burer and Monteiro, 2003](#)) allow us to reduce the original semidefinite program with $O(d^2 p^2)$ variables to the problem of finding a second-order stationary point of a related problem with only $O(d^2 p)$ variables. Since second-order stationary points can be readily found using trust-region methods ([Boumal, 2023](#)), this facilitates a useful computational reduction when p is large.

Finally, we demonstrate the utility of our theoretical results through experiments on synthetic and real-world data. We begin by proposing the IGW distance as a principled alternative to the centered kernel alignment (CKA), which is commonly used to compare neural network representations (Kornblith et al., 2019). We show that our upper and lower bounds on the IGW distance are close enough in practice to compare embedding distributions for common text datasets, which we verify to be approximately Gaussian. Our results show that IGW and CKA are positively correlated, posing the Gaussian IGW as an efficiently computable and principled alternative that would retain (and possibly improve upon) the empirical performance of CKA. Next, we model synthetic users each by an empirical measure μ_i over their text embeddings, which we approximate by a Gaussian measure $\tilde{\mu}_i$. We then cluster the users using the IGW distance between the centered versions of $\tilde{\mu}_i$, suggesting that clustering users based on their mean embedding loses useful information about higher moments of user distributions. We conclude by verifying in simulations that our Burer-Monteiro approach is faster and more numerically stable than standard interior point methods for solving the multimarginal OT problem between a large number of measures.

1.2 Related Work

IGW Alignment. Vayer (2020) introduced the inner-product variant of the GW distance, proved that the IGW distance between measures with finite second moment is finite, and derived a variational form for the IGW distance between measures with finite fourth moment. Only recently, Zhang et al. (2025) formally proved that the IGW distance is a metric on the space of probability measures over a Hilbert space with finite second moment and studied the Riemannian geometry induced by the IGW distance. Dumont et al. (2025) proved the existence of deterministic OT maps for the IGW problem between compactly supported and absolutely continuous measures in Euclidean spaces. Our work complements these theoretical results by restricting attention to Gaussian measures, which allows us to obtain closed-form expressions and efficient algorithms for computing the IGW distance and barycenter.

2-Wasserstein Distance Between Gaussians. The 2-Wasserstein distance between Gaussian measures in Euclidean space was originally studied by Knott and Smith (1984) and Givens and Shortt (1984) and is known in closed-form, giving rise to the Bures-Wasserstein geometry on the space of positive definite matrices. Their results were later extended by Gelbrich (1990) to separable Hilbert spaces. Additionally, the 2-Wasserstein barycenter between Gaussian measures can be

written as the solution of a non-linear matrix fixed-point equation, which is known to have a unique positive definite solution (Agueh and Carlier, 2011). The Bures-Wasserstein formulae and the 2-Wasserstein barycenter between Gaussians have been widely applied in the literature, including linear metric learning (Cooper, 2023), knowledge distillation in machine learning (Lv et al., 2024), style transfer for image generation (Mroueh, 2019), and covariance estimation (Han et al., 2023). Our work extends these important results by studying analogs of the Bures-Wasserstein formula for the IGW distance.

GW Alignment Between Gaussians. Salmona et al. (2022) studied the $(2, 2)$ -GW distance between Gaussian measures in Euclidean space and found an explicit solution only after restricting the optimization to Gaussian couplings; they were also able to recover the IGW distance and OT map between *centered* Gaussian measures as a corollary. Le et al. (2022) extended this work by finding closed-form expressions for the entropically regularized IGW distance and barycenter between *centered* Gaussian measures in Euclidean space, when the regularization parameter is positive. However, neither of these works treat the (unregularized) IGW alignment of uncentered Gaussian measures or general Hilbert spaces, which we address in this paper.

Multimarginal OT. The multimarginal OT problem generalizes classical OT to more than two marginal distributions. This problem was introduced for the quadratic cost by Gangbo and Świąch (1998), who focused on extending Brenier’s theorem (Brenier, 1991) to the multimarginal setting. Agueh and Carlier (2011) later related multimarginal OT to the 2-Wasserstein barycenter, by reformulating the latter as a weighted average over the optimal multimarginal coupling. Section 3 of Pass (2015) gives an overview of numerous applications of multi-marginal OT, including matching problems in economics, texture mixing in image processing, derivative pricing in finance, and incompressible fluid dynamics in engineering. In a similar vein, Beier et al. (2023) studied properties of the multimarginal GW problem between general measures and showed that it recovers the GW barycenter. Our work provides an efficient algorithm to solve the multimarginal OT problem between uncentered Gaussian measures, as well as an analytic solution to multimarginal IGW between centered Gaussians.

1.3 Notation

Let $[n] := \{1, \dots, n\}$. For $1 \leq p \leq \infty$ and probability measures μ on \mathcal{X} , let $L^p(\mu)$ be the space of real-valued measurable functions f on \mathcal{X} such that $\|f\|_{L^p(\mu)} := (\int |f(x)|^p d\mu(x))^{1/p} < \infty$, with the usual identification of functions that are equal μ -almost everywhere. We treat $\ell^2 := L^2(\mathbb{N})$ as a Hilbert space with the Euclidean inner product and write $\|\cdot\|_p$ for the p -norm on \mathbb{R}^d . We write $\mathcal{P}(\mathcal{X})$ for the class of Borel probability measures over a metric space $(\mathcal{X}, d_{\mathcal{X}})$, and let $\mathcal{P}_p(\mathcal{X}) := \{\mu \in \mathcal{P}(\mathcal{X}) : d_{\mathcal{X}}(x_0, \cdot) \in L^p(\mu) \text{ for all } x_0 \in \mathcal{X}\}$ be the subset of $\mathcal{P}(\mathcal{X})$ with finite p th moment. We use $T_{\sharp}\mu \in \mathcal{P}(\mathcal{X})$ to denote the pushforward of μ under a measurable function T , defined by $T_{\sharp}\mu(\cdot) := \mu(T^{-1}(\cdot))$.

For a Hilbert space \mathcal{H} , we use $\langle \cdot, \cdot \rangle$ and $\|x\| := \sqrt{\langle x, x \rangle}$ to denote the inner product and the induced norm, respectively. The set of trace-class operators is $\mathfrak{S}_1(\mathcal{H})$ and the set of Hilbert-Schmidt operators is $\mathfrak{S}_2(\mathcal{H})$. The set of unitary operators is designated by $\mathcal{U}(\mathcal{H})$, and we write I for the identity. We let A^* denote the adjoint of A , while A^\dagger stands for the Moore-Penrose pseudoinverse (Desoer and Whalen, 1963).

Throughout, we employ several operator and matrix norms. Let $\|A\|_{\text{op}} := \sup_{\|x\|=1} \|Ax\|$ be the operator norm. The Hilbert-Schmidt norm is denoted by $\|A\|_{\text{HS}} := (\sum_{i=1}^{\infty} \sigma_i(A)^2)^{1/2}$, where $\sigma_i(A)$ are the singular values of A . If A is trace-class, we denote its trace by $\text{tr}(A) := \sum_{i=1}^{\infty} \langle Ae_i, e_i \rangle$, where $\{e_i\}_{i=1}^{\infty}$ is any orthonormal basis of \mathcal{H} . We use \succeq to denote the Loewner order ($A \succeq 0$ means A is positive semidefinite (psd)) and \otimes to denote the tensor product. If a bounded linear operator A is self-adjoint and compact, we let $\{\lambda_i(A)\}_{i=1}^{\infty}$ denote the eigenvalues of A in non-increasing order (repeated according to multiplicity). If $A \in \mathbb{R}^{d_1 \times d_2}$ is a matrix, we write A^\top for its transpose and define its Frobenius norm as $\|A\|_F := \text{tr}(A^\top A)$.

For a probability measure on a Hilbert space $\mu \in \mathcal{P}_2(\mathcal{H})$, we write $m_\mu := \int x d\mu(x)$ for its mean. The *covariance operator* of μ is the linear operator $\Sigma_\mu : \mathcal{H} \rightarrow \mathcal{H}$ defined by the property $\langle x, \Sigma_\mu y \rangle = \int \langle x, z \rangle \langle y, z \rangle d\mu(z)$. Given $\mu_1, \mu_2 \in \mathcal{P}_2(\mathcal{H})$ and a coupling $\pi \in \Pi(\mu_1, \mu_2)$, the *cross-covariance operator* is the linear operator $\Sigma_\pi^\times : \mathcal{H} \rightarrow \mathcal{H}$ defined by the property $\langle x, \Sigma_\pi^\times y \rangle = \int \langle x, r \rangle \langle y, s \rangle d\pi(r, s)$; this corresponds to the upper-right block of Σ_π written as a block operator on $\mathcal{H} \oplus \mathcal{H}$ (where \oplus denotes the direct sum). We write $\mathcal{N}(m, \Sigma)$ for the Gaussian measure on \mathcal{H} with mean m and covariance operator Σ . Write $\mathcal{G}(\mathcal{H})$ for the set of Gaussian measures on \mathcal{H} , and let $\mathcal{G}_0(\mathcal{H}) = \{\mu \in \mathcal{G}(\mathcal{H}) : m_\mu = 0\}$ be the set of centered Gaussians. A brief exposition on probability theory over Hilbert spaces is provided in [Appendix F](#).

2 Background

OT, barycenter, and multimarginal. The Kantorovich OT problem between probability distributions $\mu_1 \in \mathcal{P}(\mathcal{X}_1)$ and $\mu_2 \in \mathcal{P}(\mathcal{X}_2)$ with cost function $c : \mathcal{X}_1 \times \mathcal{X}_2 \rightarrow \mathbb{R}$ is given by (Kantorovich, 1942; Villani, 2003):

$$\text{OT}_c(\mu_1, \mu_2) := \inf_{\pi \in \Pi(\mu_1, \mu_2)} \int c(x, y) d\pi(x, y),$$

where $\Pi(\mu_1, \mu_2) := \{\pi \in \mathcal{P}(\mathcal{X}_1 \times \mathcal{X}_2) : \pi(\cdot \times \mathcal{X}_2) = \mu_1, \pi(\mathcal{X}_1 \times \cdot) = \mu_2\}$ is the set of couplings of μ_1, μ_2 . Intuitively, the Kantorovich problem searches for a (randomized) transportation plan π that reshapes μ_1 into μ_2 that minimizes the expected transportation cost. The common choice $\mathcal{X}_1 = \mathcal{X}_2 = \mathbb{R}^d$ under the quadratic cost $\|x - y\|_2^2$ yields the *2-Wasserstein distance*

$$W_2(\mu_1, \mu_2) := \text{OT}_{\|\cdot\|^2}(\mu_1, \mu_2)^{1/2} = \inf_{\pi \in \Pi(\mu_1, \mu_2)} \|X - Y\|_{L^2(\pi)} \quad (1)$$

between measures $\mu_1, \mu_2 \in \mathcal{P}_2(\mathbb{R}^d)$. If μ_1 and μ_2 are also absolutely continuous with respect to the Lebesgue measure, a landmark theorem due to Brenier (1991) shows that a unique optimal plan for (1) is given by $\pi = (I, \nabla\varphi)_\# \mu_1$ for a proper lower semi-continuous convex function $\varphi : \mathbb{R}^d \rightarrow \mathbb{R}$. In other words, the optimal plan is induced by a deterministic transport map $T = \nabla\varphi$, given as the gradient of a convex function (i.e., monotone for $d = 1$ and \tilde{c} -cyclically monotone in general (Villani, 2003, Chapter 2)). The Wasserstein distance metrizes weak convergence of probability measures and gives rise to a rich Riemannian geometry on the so-called 2-Wasserstein space $(\mathcal{P}_2(\mathbb{R}^d), W_2)$ (Villani, 2003, Chapter 8). Further background related to OT is provided in Appendix D.1.

The Wasserstein geometry induces a meaningful notion of an average of collections of probability distributions, under the Wasserstein barycenter framework. For $\rho \in \mathcal{P}(\mathcal{P}_2(\mathbb{R}^d))$, the ρ -weighted 2-Wasserstein barycenter is defined as the Frechet mean under W_2 :

$$\bar{\mu} \in \arg \min_{\mu \in \mathcal{P}_2(\mathbb{R}^d)} \int W_2(\mu, \nu)^2 d\rho(\nu).$$

The 2-Wasserstein barycenter exists and is unique (Agueh and Carlier, 2011), and is usually computed using fixed-point iteration or entropic regularization (Peyré and Cuturi, 2019, Section 9.2).

Gangbo and Świąch (1998) studied the related multimarginal OT problem

$$\inf_{\pi \in \Pi(\mu_1, \dots, \mu_p)} \int \sum_{i=1}^p \sum_{j=i+1}^p \|x_i - x_j\|_2^2 d\pi(x_1, \dots, x_p), \quad (2)$$

where $\Pi(\mu_1, \dots, \mu_p)$ is the set of p -plans, i.e., joint distributions $\pi \in \mathcal{P}(\mathcal{X}_1 \times \dots \times \mathcal{X}_p)$ that have μ_i as their i th marginal, for all $i = 1, \dots, p$. Gangbo and Świąch (1998) proved that if μ_1, \dots, μ_p

are absolutely continuous with respect to the Lebesgue measure, then there exists a unique optimal coupling π for the multimarginal problem. The barycenter and multimarginal OT problem are connected by the following result.

Proposition 2.1 (Agueh and Carlier (2011), Proposition 4.2). *Suppose that $\rho \in \mathcal{P}(\mathcal{P}_2(\mathbb{R}^d))$ has $\text{supp}(\rho) = \{\mu_1, \dots, \mu_p\}$ for absolutely continuous measures μ_i . Define*

$$g(x_{\mu_1}, \dots, x_{\mu_p}) := \int x_\nu d\rho(\nu)$$

for $x_{\mu_1}, \dots, x_{\mu_p} \in \mathbb{R}^d$. If $\pi \in \Pi(\mu_1, \dots, \mu_p)$ solves the multimarginal OT problem between μ_1, \dots, μ_p , then $g_\# \pi$ is a ρ -weighted 2-Wasserstein barycenter.

The Gaussian case: Bures-Wasserstein distance. As an important special case of (1), suppose that $\mu_1 = \mathcal{N}(m_1, \Sigma_1)$ and $\mu_2 = \mathcal{N}(m_2, \Sigma_2)$ are nondegenerate Gaussian measures, where $\Sigma_1 \succ 0$ and $\Sigma_2 \succ 0$. Brenier's theorem then implies that the optimal coupling between Gaussian measures $\pi = (I, T)_\# \mu_1$ must be supported on the graph of a deterministic function $T : \mathbb{R}^d \rightarrow \mathbb{R}^d$. Knott and Smith (1984) and Givens and Shortt (1984) prove the formula for the OT map

$$T(x) = \Sigma_1^{-1/2} (\Sigma_1^{1/2} \Sigma_2 \Sigma_1^{1/2})^{1/2} \Sigma_1^{-1/2} (x - m_1) + m_2, \quad (3)$$

resulting in the *Bures-Wasserstein* formula for the 2-Wasserstein distance

$$W_2(\mu_1, \mu_2) = \sqrt{\|m_1 - m_2\|_2^2 + \text{tr} \left(\Sigma_1 + \Sigma_2 - 2 (\Sigma_1^{1/2} \Sigma_2 \Sigma_1^{1/2})^{1/2} \right)}, \quad (4)$$

which yields the Bures-Wasserstein geometry, induced by $\text{BW}(\Sigma_1, \Sigma_2) := W_2(\mathcal{N}(0, \Sigma_1), \mathcal{N}(0, \Sigma_2))$ on the space of symmetric $d \times d$ positive definite matrices.

Beyond the quadratic bimarginal case, another instance that notably simplifies under the Gaussian setting is the Wasserstein barycenter. Agueh and Carlier (2011) proved that if $\text{supp}(\rho) = \{\mu_1, \dots, \mu_p\}$, where $\mu_i = \mathcal{N}(0, \Sigma_i)$ and $\Sigma_i \succ 0$ are nondegenerate Gaussians for $i \in [p]$, then the barycenter is Gaussian $\mathcal{N}(0, \Sigma)$ whose covariance matrix Σ is the unique positive definite fixed-point of the equation

$$\Sigma = \int (\Sigma^{1/2} \Sigma_\nu \Sigma^{1/2})^{1/2} d\rho(\nu). \quad (5)$$

Equations (4) and (5) are the cornerstones for various recent works studying theory and practical applications of closed-form solutions to Gaussian OT (Mroueh, 2019; Cooper, 2023; Han et al., 2023; Lv et al., 2024), motivating our study of various OT problems between Gaussians.

GW alignment. The Wasserstein distance inherently assumes distributions supported on a shared space, as the cost is given in terms of the base distance. The *Gromov-Wasserstein (GW) distances* provide a framework for quantifying discrepancy between distributions on distinct spaces ($\mu_1 \in \mathcal{P}(\mathcal{X})$ and $\mu_2 \in \mathcal{P}(\mathcal{Y})$). This is done by minimizing distortion between intrinsic similarity functions on each space ($k_{\mathcal{X}}$ and $k_{\mathcal{Y}}$ on \mathcal{X} and \mathcal{Y} respectively):

$$\begin{aligned} \text{GW}_2(\mu_1, \mu_2) &:= \left(\inf_{\pi \in \Pi(\mu_1, \mu_2)} \int (k_{\mathcal{X}}(x, x') - k_{\mathcal{Y}}(y, y'))^2 d(\pi \otimes \pi)(x, y, x', y') \right)^{1/2} \\ &= \|k_{\mathcal{X}}(X, X') - k_{\mathcal{Y}}(Y, Y')\|_{L^2(\pi \otimes \pi)}. \end{aligned}$$

If \mathcal{X} and \mathcal{Y} are Hilbert spaces, setting $k_{\mathcal{X}}(x, x') = \langle x, x' \rangle$ and $k_{\mathcal{Y}}(y, y') = \langle y, y' \rangle$ yields the *inner product Gromov-Wasserstein (IGW) distance*. If \mathcal{H} is a Hilbert space, the IGW distance is a metric on the quotient space of $\mathcal{P}_2(\mathcal{H})$, modulo equivalence of measures separated almost surely by a unitary transformation (Zhang et al., 2025, Proposition 3.1). The extension of the GW framework to the multimarginal setting was recently considered in Beier et al. (2023). That work also established the relationship between multimarginal GW and the GW barycenter, analogous to Proposition 2.1 in the Wasserstein case.

Previous work studies the IGW distance and barycenter between Gaussian measures, but existing results are limited to centered Gaussians in finite dimensions. For bimarginal IGW, Salmona et al. (2022) show that

$$\text{IGW}(\mathcal{N}(0, \Sigma_1), \mathcal{N}(0, \Sigma_2)) = \sum_{i=1}^{\infty} (\lambda_k(\Sigma_1) - \lambda_k(\Sigma_2))^2,$$

where $\lambda_k(\Sigma_i)$ denotes the k th largest eigenvalue of Σ_i . Building on this result, Le et al. (2022) further provided a formula for the IGW barycenter. In this work, we extend these results to significantly broaden their practical applicability. Further exposition on GW distances and related results are collected in Appendix D.2. We also provide some background on Riemannian optimization and the Stiefel manifold in Appendix E.

3 IGW Alignment Between Gaussian Measures

This section studies the IGW alignment problem between Gaussian measures on general Hilbert spaces. We treat the bimarginal setting, analyzing both the alignment cost and optimal plan, and build on it to resolve the IGW barycenter. Throughout this section, assume that \mathcal{H} is a separable Hilbert space.

3.1 IGW Distance and Optimal Coupling

Our first result provides a near closed-form expression for the IGW distance and optimal coupling between general (possibly uncentered) Gaussian measures, up to a quadratic optimization over unitary operators. Following this statement, we derive tight analytic upper and lower bounds on the optimal value of that unitary optimization.

Theorem 3.1 (IGW between Gaussians). *Let $\mu_1 = \mathcal{N}(m_1, \Sigma_1)$ and $\mu_2 = \mathcal{N}(m_2, \Sigma_2)$ be Gaussian measures on \mathcal{H} . For a total orthonormal set $\{e_k\}_{k \in \mathbb{N}}$, let $\Sigma_i = Q_i \Lambda_i Q_i^*$ be the spectral decomposition of Σ_i with respect to $\{e_k\}_{k \in \mathbb{N}}$, where $\Lambda_i = \sum_{k=1}^{\infty} \lambda_k(\Sigma_i) e_k \otimes e_k$ and $Q_i \in \mathcal{U}(\mathcal{H})$ (for $i \in [2]$). Setting $\tilde{m}_i := Q_i^* m_i$ for $i \in [2]$, define*

$$\gamma(\mu_1, \mu_2) := \sup_{C \in \mathcal{U}(\mathcal{H})} \left\{ \text{tr}(\Lambda_1 C^* \Lambda_2 C) + 2 \left\langle C \Lambda_1^{1/2} \tilde{m}_1, \Lambda_2^{1/2} \tilde{m}_2 \right\rangle \right\}. \quad (6)$$

The supremum above is attained at some $C \in \mathcal{U}(\mathcal{H})$ and the IGW distance between μ_1 and μ_2 is

$$\text{IGW}(\mu_1, \mu_2) = \sqrt{\text{tr}(\Lambda_1^2) + \text{tr}(\Lambda_2^2) + 2 \langle \tilde{m}_1, \Lambda_1 \tilde{m}_1 \rangle + 2 \langle \tilde{m}_2, \Lambda_2 \tilde{m}_2 \rangle + (\|\tilde{m}_1\|^2 - \|\tilde{m}_2\|^2)^2 - 2\gamma(\mu_1, \mu_2)}.$$

Assuming without loss of generality (w.l.o.g.) that $\text{rank}(\Sigma_1) \geq \text{rank}(\Sigma_2)$ and defining $T : \mathcal{H} \rightarrow \mathcal{H}$ by $T(x) = m_2 + Q_2 \Lambda_2^{1/2} C^* \Lambda_1^{1/2} Q_1^*(x - m_1)$, an optimal IGW coupling π between μ_1 and μ_2 is

$$\pi = (I, T)_\# \mu_1 = \mathcal{N} \left(\begin{bmatrix} m_1 \\ m_2 \end{bmatrix}, \begin{bmatrix} \Sigma_1 & Q_1 \Lambda_1^{1/2} C \Lambda_2^{1/2} Q_2^* \\ Q_2 \Lambda_2^{1/2} C^* \Lambda_1^{1/2} Q_1^* & \Sigma_2 \end{bmatrix} \right).$$

The proof of [Theorem 3.1](#), deferred to [Appendix A](#), observes that, upon expanding the IGW cost, the resulting optimization problem only depends on the covariance of π . Thus, we may restrict to jointly Gaussian couplings π without changing the optimal value. Rewriting the constraints using the Schur complement condition for positive semidefiniteness, we arrive at an optimization problem over contractive operators. Using Bauer's maximum principle, we then argue that the optimum is attained on the boundary of the feasible set, resulting in the unitary optimization $\gamma(\mu_1, \mu_2)$.

Remark 3.1 (Finite-dimensional case). If $\mu_i \in \mathcal{P}_2(\mathbb{R}^{d_i})$, for $i \in [2]$, with $d_1 \geq d_2$ w.l.o.g., the formula from (6) further simplifies to

$$\gamma(\mu_1, \mu_2) = \sup_{C \in \text{St}(d_1, d_2)} \left\{ \text{tr}(\Lambda_1 C \Lambda_2 C^\top) + 2 \left\langle \Lambda_1^{1/2} \tilde{m}_1, C \Lambda_2^{1/2} \tilde{m}_2 \right\rangle \right\},$$

where $\Lambda_i = \text{diag}(\lambda_1(\Sigma_i), \dots, \lambda_{d_i}(\Sigma_i))$ for $i \in [2]$ and $\text{St}(d_1, d_2) := \{C \in \mathbb{R}^{d_1 \times d_2} : C^\top C = I\}$ is the *Stiefel manifold* of orthonormal d_2 -frames in \mathbb{R}^{d_1} . Since $\text{St}(d_1, d_2)$ is a smooth, compact Riemannian

manifold, we may use standard manifold optimization techniques to solve this problem in practice (Absil et al., 2008). Due to the non-convexity of the objective, iterative manifold optimization schemes could converge to local optima, which would only provide a lower bound on $\gamma(\mu_1, \mu_2)$. Theorem 3.2, stated next, provides analytic upper and lower bounds on $\gamma(\mu_1, \mu_2)$ that require no optimization and hold in general Hilbert spaces.

The following bounds on the Gaussian IGW distance follow by inspecting $\gamma(\mu_1, \mu_2)$ from (6) and identifying closed-form solutions to each of the two added terms in the objective, separately. The resulting expressions are given in terms of the means and covariance operators of μ_1, μ_2 , and are thus computable.

Theorem 3.2 (Analytic bounds). *Under the setting of Theorem 3.1, define*

$$\xi(\mu_1, \mu_2) := \sum_{k=1}^{\infty} (\lambda_k(\Lambda_1) - \lambda_k(\Lambda_2))^2 + 2\langle \tilde{m}_1, \Lambda_1 \tilde{m}_1 \rangle + 2\langle \tilde{m}_2, \Lambda_2 \tilde{m}_2 \rangle + (\|\tilde{m}_1\|^2 - \|\tilde{m}_2\|^2)^2.$$

Then IGW distance between $\mu_1 = \mathcal{N}(m_1, \Sigma_1)$ and $\mu_2 = \mathcal{N}(m_2, \Sigma_2)$ satisfies

$$\xi(\mu_1, \mu_2) - 4\|\Lambda_1^{1/2}\tilde{m}_1\|\|\Lambda_2^{1/2}\tilde{m}_2\| \leq \text{IGW}(\mu_1, \mu_2)^2 \leq \xi(\mu_1, \mu_2) - 4\langle \Lambda_1^{1/2}\tilde{m}_1, \Lambda_2^{1/2}\tilde{m}_2 \rangle. \quad (7)$$

In fact, the upper bound above holds for all $\mu_i \in \mathcal{P}_2(\mathcal{H})$ with mean m_i and covariance Σ_i , for $i \in [2]$.

Inequality (7) bounds the squared IGW distance between Gaussians within the Cauchy-Schwarz gap between $\langle \Lambda_1^{1/2}\tilde{m}_1, \Lambda_2^{1/2}\tilde{m}_2 \rangle$ and $\|\Lambda_1^{1/2}\tilde{m}_1\|\|\Lambda_2^{1/2}\tilde{m}_2\|$. For the lower bound, observe that the first term in $\gamma(\mu_1, \mu_2)$ is maximized by $C = I$ due to the von Neumann trace inequality, while the second term is maximized by

$$C = \frac{(\Lambda_2^{1/2}\tilde{m}_2) \otimes (\Lambda_1^{1/2}\tilde{m}_1)}{\|\Lambda_2^{1/2}\tilde{m}_2\|\|\Lambda_1^{1/2}\tilde{m}_1\|}$$

due to the Cauchy-Schwarz inequality (subject to the constraint). Maximizing each term separately yields an upper bound on $\gamma(\mu_1, \mu_2)$, and hence a lower bound on the IGW distance. For the upper bound, we simply set $C = I$. The fact that the upper bound holds for general (not necessarily Gaussian) probability measures over \mathcal{H} , with matched first and second moments, is a consequence of the following result.

Corollary 3.1 (Gaussian bound). *If $\mu_i \in \mathcal{P}_2(\mathcal{H})$ for $i \in [2]$, we have*

$$\text{IGW}(\mu_1, \mu_2) \leq \text{IGW}(\mathcal{N}(m_{\mu_1}, \Sigma_{\mu_1}), \mathcal{N}(m_{\mu_2}, \Sigma_{\mu_2})).$$

This corollary follows from the proof of [Theorem 3.1](#), which shows that the IGW distance between two Gaussians is also an upper bound on the IGW distance between *any* two measures in $\mathcal{P}_2(\mathcal{H})$ with the same covariance. This is another motivation for using Gaussian measures as a proxy for more general measures. Lastly, we highlight two cases where $\gamma(\mu_1, \mu_2)$ is solvable in closed-form, leading to an analytic expression for the IGW distance between Gaussians.

Corollary 3.2 (Analytic solutions). *The following hold:*

- (i) (Co-centered Gaussians) *Under the setting of [Theorem 3.1](#), suppose that $\Lambda_1^{1/2}\tilde{m}_1 = \alpha \Lambda_2^{1/2}\tilde{m}_2$ for some $\alpha \geq 0$. Then*

$$\text{IGW}(\mathcal{N}(m_1, \Sigma_1), \mathcal{N}(m_2, \Sigma_2)) = \sqrt{\xi(\mu_1, \mu_2) + \|\Lambda_1^{1/2}\tilde{m}_1\| \|\Lambda_2^{1/2}\tilde{m}_2\|},$$

where $\xi(\mu_1, \mu_2)$ is given in the statement of [Theorem 3.2](#).

- (ii) (Univariate Gaussians) *The IGW distance between Gaussians on \mathbb{R} is given by*

$$\text{IGW}(\mathcal{N}(m_1, \sigma_1^2), \mathcal{N}(m_2, \sigma_2^2)) = \sqrt{(\sigma_1^2 - \sigma_2^2)^2 + (m_1^2 - m_2^2)^2 + 2(\sigma_1|m_1| - \sigma_2|m_2|)^2}.$$

The expression for the first case follows from [Theorem 3.2](#), since the upper and lower bounds on the IGW distance coincide under the co-centering condition $\Lambda_1^{1/2}\tilde{m}_1 = \alpha \Lambda_2^{1/2}\tilde{m}_2$, which corresponds to the equality case of the Cauchy-Schwarz inequality. This result generalizes the formula of [Salmona et al. \(2022\)](#) and [Le et al. \(2022\)](#) to (for example) the case where only one of the measures is centered, and further allows us to handle the case of general separable Hilbert spaces. The formula for univariate Gaussians is a direct consequence of [Theorem 3.1](#) by observing that the only unitary operators on \mathbb{R} are ± 1 , which enables resolving $\gamma(\mu_1, \mu_2)$ in closed-form. The univariate formula can be used to efficiently estimate the *sliced* GW distance between Gaussians ([Vayer et al., 2019](#)).

Remark 3.2 (Gromov-Bures-Wasserstein distance). By (i) of [Corollary 3.2](#), $(\mathcal{G}_0(\mathcal{H}), \text{IGW})$ is isometric to the nonnegative orthant of the Hilbert space ℓ^2 . Defining $\mathfrak{C}(\mathcal{H}) := \{\Sigma \in \mathfrak{S}_1(\mathcal{H}) : \Sigma = \Sigma^* \succ 0\}$ as the set of non-degenerate covariance operators, we refer to

$$\text{GBW}(\Sigma_1, \Sigma_2) := \text{IGW}(\mathcal{N}(0, \Sigma_1), \mathcal{N}(0, \Sigma_2)) = \left(\sum_{k=1}^{\infty} (\lambda_k(\Sigma_1) - \lambda_k(\Sigma_2))^2 \right)^{1/2}$$

as the *Gromov-Bures-Wasserstein (GBW) distance* between $\Sigma_1, \Sigma_2 \in \mathfrak{C}(\mathcal{H})$. Although the IGW distance is not a geodesic distance in general, one interesting avenue for future work is to study the Riemannian geometry induced by the intrinsic version of this metric ([Zhang et al., 2025](#), Definition

5.2). Essentially, the GBW distance orthogonally aligns the eigenspaces of Σ_1 and Σ_2 so that they are simultaneously diagonalizable, and then computes the Hilbert-Schmidt distance between the resulting diagonal operators. This is in contrast to the usual Bures-Wasserstein distance

$$\text{BW}(\Sigma_1, \Sigma_2) := W_2(\mathcal{N}(0, \Sigma_1), \mathcal{N}(0, \Sigma_2)) = \left(\text{tr}(\Sigma_1) + \text{tr}(\Sigma_2) - 2 \text{tr} \left(\left(\Sigma_1^{1/2} \Sigma_2 \Sigma_1^{1/2} \right)^{1/2} \right) \right)^{1/2}$$

from (4), which is a Riemannian metric on $\mathfrak{C}(\mathcal{H})$ defined using the quadratic Wasserstein distance between centered Gaussians (Givens and Shortt, 1984; Knott and Smith, 1984).

We conclude this section with the following example that provides geometric intuition about IGW alignment between Gaussian measures in \mathbb{R}^2 .

Example 3.1 (Gaussians on the plane). By Corollary 3.1, note that any choice of $C \in \mathcal{U}(\mathcal{H})$ in Theorem 3.1 (such as one obtained by a manifold optimization scheme) yields a valid upper bound on the IGW distance. Initializing such a scheme at, e.g., $C = I$, and following the negative gradient allows us to tighten the upper bound in Theorem 3.2.

Now, we can plot the displacement interpolation between two univariate Gaussians under the IGW distance and W_2 distance in Figure 2. Recall that for an optimal OT/IGW map T , the displacement interpolation between μ_1 and μ_2 is defined by $((1-t)I + tT)_\# \mu_1$, for $t \in [0, 1]$. The IGW optimal map is given in Theorem 3.1; to estimate C , we use Riemannian gradient descent (RGD) with a simple adaptive step size for a maximum of 50 iterations or until the norm of the Riemannian gradient is less than 10^{-2} . The 2-Wasserstein OT map is given by (3).

Figure 2 compares the two interpolations, showing that the IGW map prefers to rotate the measures, while the 2-Wasserstein OT map moves mass in straight lines. The IGW distance is not invariant to translation of both measures, although the Wasserstein distance is; we depict this in Figure 2 by plotting the displacement interpolation between translated versions of the measures. Observe that the IGW map rotates the measure around the origin, while the optimal 2-Wasserstein map transports mass in straight lines like before.

3.2 IGW Barycenter Between Centered Gaussians

In this section, we generalize the formula of Le et al. (2022) for the IGW barycenter between centered Gaussian measures. First, we define the notion of an IGW barycenter as any Frechét mean under the IGW distance (analogously to the 2-Wasserstein barycenter of Agueh and Carlier (2011)).

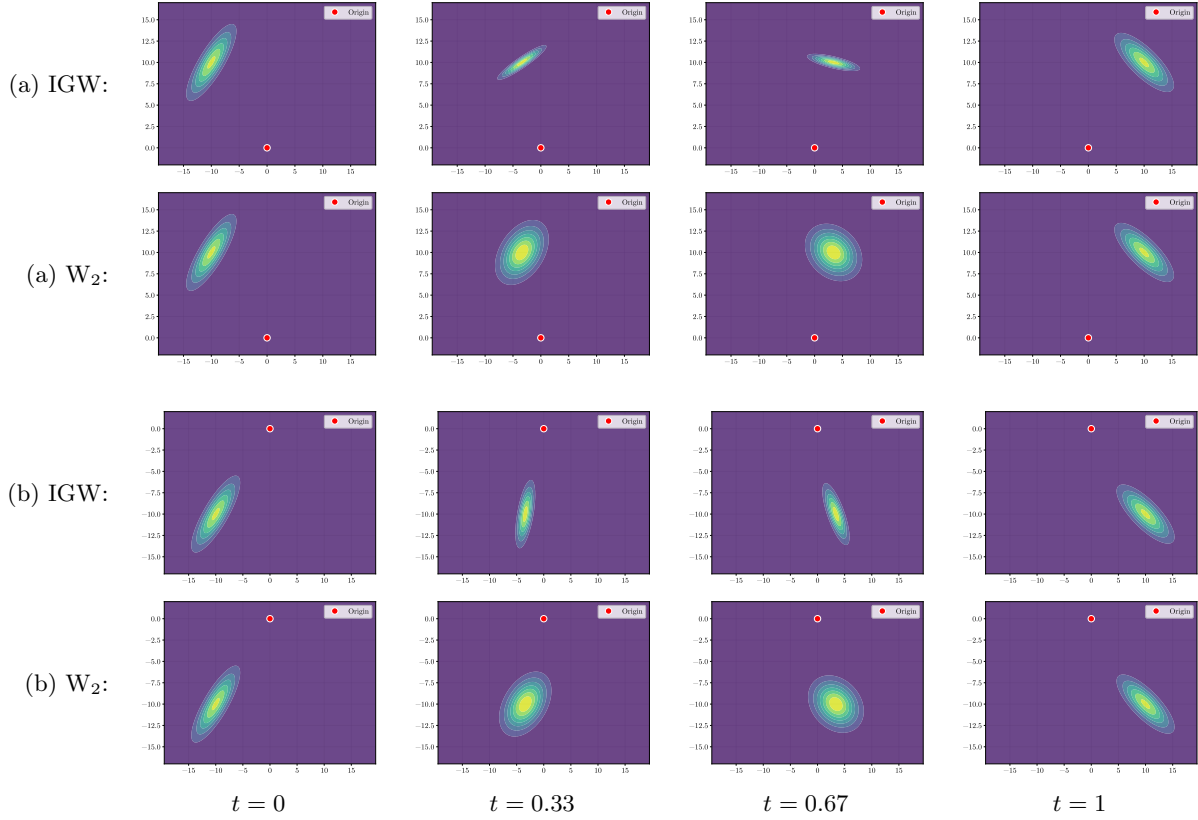


Figure 2: *Comparison of displacement interpolations between two Gaussian distributions (origin marked in red). (a) has the origin at the bottom and (b) has the origin at the top; note that the IGW interpolation prefers to rotate the measures around the origin while the W_2 interpolation is invariant to translation of both measures. Top row of (a) and (b): IGW displacement interpolation between two Gaussians with OT map estimated using RGD. Bottom row of (a) and (b): 2-Wasserstein displacement interpolation with OT map from the Bures-Wasserstein formula in (3).*

Definition 3.1 (IGW barycenter). Suppose that $\rho \in \mathcal{P}(\mathcal{P}_2(\mathcal{H}))$, where $\mathcal{P}_2(\mathcal{H})$ is equipped with the smallest σ -algebra so that $\mu \mapsto \mu(B)$ is measurable for all Borel sets $B \in \mathcal{B}(\mathcal{H})$. A measure $\bar{\mu} \in \mathcal{P}_2(\mathcal{H})$ is a ρ -weighted IGW barycenter if

$$\bar{\mu} \in \arg \min_{\mu \in \mathcal{P}_2(\mathcal{H})} \left\{ \int \text{IGW}(\mu, \nu)^2 d\rho(\nu) \right\}.$$

Using this definition, we can solve the IGW barycenter problem when ρ is supported on the space $\mathcal{G}_0(\mathcal{H})$ of centered Gaussian measures over \mathcal{H} . We have the following representation.

Proposition 3.3 (Gaussian IGW barycenter). Suppose that $\rho \in \mathcal{P}(\mathcal{P}_2(\mathcal{H}))$ has $\text{supp}(\rho) \subseteq \mathcal{G}_0(\mathcal{H})$ and the map $(\mu \mapsto \lambda_k(\Sigma_\mu)) \in L^2(\rho)$, for all $\mu \in \mathcal{G}_0$. For any fixed total orthonormal set $\{e_k\}_{k \in \mathbb{N}}$ of \mathcal{H} , the measure $\mathcal{N}(0, \Sigma)$ with covariance operator

$$\Sigma := \sum_{k=1}^{\infty} \left(\int \lambda_k(\Sigma_\nu) d\rho(\nu) \right) e_k \otimes e_k,$$

is a ρ -weighted IGW barycenter.

A special case of this result occurs when ρ is a finitely-supported measure over centered Gaussian measures, each over a Euclidean space. Restricting the barycenter to lie in $\mathcal{P}_2(\mathbb{R}^d)$ for some $d \in \mathbb{N}$, we recover the formula of [Le et al. \(2022\)](#).

Remark 3.3 (Finite-dimensional IGW barycenter). In the setting of [Proposition 3.3](#), suppose that $\text{supp}(\rho) = \{\mu_1, \dots, \mu_p\}$, where $\mu_i = \mathcal{N}(0, \Sigma_i)$ and $\text{rank}(\Sigma_i) = d_i$ for $i \in [p]$. Further, suppose that we restrict the optimization in [Definition 3.1](#) to be over $\mu \in \mathcal{P}_2(\mathbb{R}^d)$ instead of over all of $\mathcal{P}_2(\mathcal{H})$; this is called a *fixed-support barycenter* in [Beier et al. \(2023\)](#). Define $d_{\mu_i} := d_i$ for $i \in [p]$. Then, $\mathcal{N}(0, \Sigma)$ is a ρ -weighted fixed-support IGW barycenter, where

$$\Sigma := \text{diag} \left(\int \lambda_1(\Sigma_\nu) \mathbf{1}_{1 \leq d_\nu} d\rho(\nu), \dots, \int \lambda_d(\Sigma_\nu) \mathbf{1}_{d \leq d_\nu} d\rho(\nu) \right).$$

Setting $d \geq \max_{i \in [p]} d_i$ recovers the same value of the objective function as the arbitrary-support barycenter from [Proposition 3.3](#).

To elucidate the action of the IGW barycenter found in [Proposition 3.3](#), we conclude this section with the following example.

Example 3.2 (IGW barycenter preserves geometry). Suppose we have input measures $\mu_i =$

$\mathcal{N}(0, \Sigma_i)$ for $i \in [2]$ on \mathbb{R}^2 , where

$$\begin{aligned}\Sigma_1 &:= \begin{bmatrix} \sqrt{3}/2 & 1/2 \\ -1/2 & \sqrt{3}/2 \end{bmatrix} \begin{bmatrix} 100 & 0 \\ 0 & 10 \end{bmatrix} \begin{bmatrix} \sqrt{3}/2 & 1/2 \\ -1/2 & \sqrt{3}/2 \end{bmatrix}^\top, \\ \Sigma_2 &:= \begin{bmatrix} \sqrt{2}/2 & -\sqrt{2}/2 \\ \sqrt{2}/2 & \sqrt{2}/2 \end{bmatrix} \begin{bmatrix} 100 & 0 \\ 0 & 10 \end{bmatrix} \begin{bmatrix} \sqrt{2}/2 & -\sqrt{2}/2 \\ \sqrt{2}/2 & \sqrt{2}/2 \end{bmatrix}^\top,\end{aligned}$$

and let $\rho = \text{Unif}(\{\mu_1, \mu_2\})$. The ρ -weighted 2-Wasserstein barycenter (which can be computed as the solution of the fixed-point equation in Theorem 6.1 of [Agueh and Carlier \(2011\)](#)) does not preserve the shape of the input measures, but the ρ -weighted IGW barycenter (computed from [Proposition 3.3](#)) does. We display contour plots of both barycenters in [Figure 3](#) to illustrate this.

The 2-Wasserstein barycenter minimizes a weighted combination of 2-Wasserstein distances to the μ_i , even if the shape of the barycenter needs to be completely different than those of the input measures. On the other hand, the IGW barycenter is orthogonally invariant and incurs no cost from rotations. In this sense, the IGW barycenter is an average with respect to the task of *alignment*, whereas the 2-Wasserstein barycenter is an average with respect to the task of *transport*.

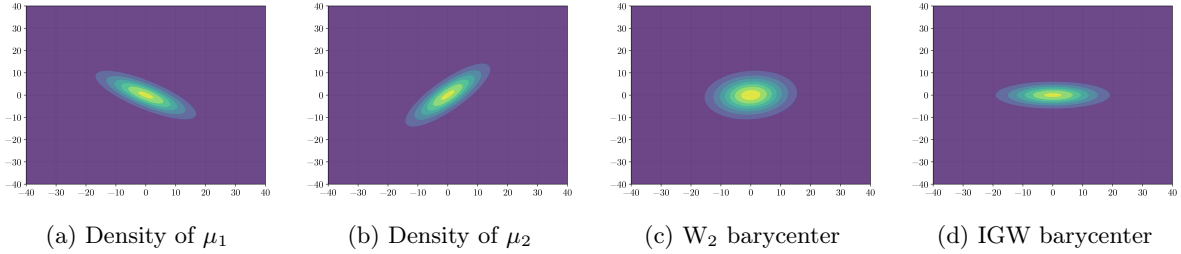


Figure 3: *Contour plots of the ρ -weighted 2-Wasserstein barycenter and ρ -weighted IGW barycenter. The 2-Wasserstein barycenter does not preserve the covariance structure of the input measures, but the IGW barycenter naturally does.*

While the results in this section pertained to the bi-marginal IGW problem, we now discuss the multimarginal OT problem and derive new results, under both the IGW cost and under the 2-Wasserstein cost.

4 Multimarginal Problems Between Gaussian Measures

In this section, we consider a multimarginal version of the IGW problem, as well as the related multimarginal 2-Wasserstein problem introduced in [Gangbo and Święch \(1998\)](#), between Gaussian measures. All proofs are deferred to [Appendix A](#).

4.1 Multimarginal IGW

Given $\mu_1, \dots, \mu_p \in \mathcal{P}_2(\mathcal{H})$ for a separable Hilbert space \mathcal{H} , the multimarginal IGW problem is

$$\inf_{\pi \in \Pi(\mu_1, \dots, \mu_p)} \int \sum_{i=1}^p \sum_{j=i+1}^p (\langle x_i, x'_i \rangle - \langle x_j, x'_j \rangle)^2 d(\pi \otimes \pi)(x_1, \dots, x_p, x'_1, \dots, x'_p).$$

Note that the cost is now the sum of pairwise bi-marginal IGW costs, which is analogous to the multimarginal 2-Wasserstein problem of [Gangbo and Świąch \(1998\)](#) shown in (2). When the inputs to the problem are centered Gaussian measures, we obtain the following closed-form solution.

Theorem 4.1 (Multimarginal IGW between Gaussians). *Suppose that $\mu_i = \mathcal{N}(0, \Sigma_i)$ are centered Gaussian measures on a separable Hilbert space \mathcal{H} , for $i \in [p]$. Let $\{v_k\}_{k \in \mathbb{N}}$ be any total orthonormal set and $\Sigma_i = Q_i \Lambda_i Q_i^*$ be the spectral decomposition of Σ_i , where $\Lambda_i = \sum_{k=1}^{\infty} \lambda_k(\Sigma_i) v_k \times v_k$ and $Q_i \in \mathcal{U}(\mathcal{H})$ (for $i \in [2]$). Then, the measure*

$$\mathcal{N} \left(0, \begin{bmatrix} \Sigma_1 & Q_1 \Lambda_1^{1/2} \Lambda_2^{1/2} Q_2^* & \cdots & Q_1 \Lambda_1^{1/2} \Lambda_p^{1/2} Q_p^* \\ Q_2 \Lambda_2^{1/2} \Lambda_1^{1/2} Q_1^* & \Sigma_2 & \cdots & Q_2 \Lambda_2^{1/2} \Lambda_p^{1/2} Q_p^* \\ \vdots & \vdots & \ddots & \vdots \\ Q_p \Lambda_p^{1/2} \Lambda_1^{1/2} Q_1^* & Q_p \Lambda_p^{1/2} \Lambda_2^{1/2} Q_2^* & \cdots & \Sigma_p \end{bmatrix} \right)$$

solves the multimarginal IGW problem between μ_1, \dots, μ_p . Here, the above matrix is to be interpreted as a block operator on $\oplus_{i=1}^p \mathcal{H}$ ([Bikchentaev et al., 2024](#), Section 1.6).

The proof of this result follows from the fact that the cross-covariance matrix $Q_i \Lambda_i \Lambda_j Q_j^*$ optimizes the pairwise IGW cost between μ_i and μ_j subject to a looser bi-marginal constraint, so it suffices to check that the resulting block operator is positive semidefinite. The full proof can be found in [Appendix A](#).

Essentially, this result implies that the multimarginal IGW alignment problem between centered Gaussian measures is solved by orthogonally transforming each measure so that they are all simultaneously diagonalizable, and then coupling them so that their corresponding eigenvectors are maximally correlated. In [Appendix B](#), we use [Theorem 4.1](#) to recover a special case of the IGW Gaussian barycenter formula of [Proposition 3.3](#). Next, we discuss the multimarginal OT problem between Gaussian measures under the quadratic Wasserstein cost.

4.2 Multimarginal Optimal Transport

Recall the multimarginal OT problem of [Gangbo and Świąch \(1998\)](#) with pairwise quadratic cost:

$$\inf_{\pi \in \Pi(\mu_1, \dots, \mu_p)} \int \sum_{i=1}^p \sum_{j=i+1}^p \|x_i - x_j\|_2^2 d\pi(x_1, \dots, x_p). \quad (8)$$

For Gaussians, we can rewrite the multimarginal OT problem with pairwise quadratic costs from (2) as a semidefinite program. Exploring its structure reveals that it can be solved efficiently via a rank-deficiency constraint.

Theorem 4.2 (Multimarginal OT between Gaussians). *Suppose that $\mu_i = \mathcal{N}(m_i, \Sigma_i)$ are Gaussian measures on \mathbb{R}^d with $\Sigma_i \succ 0$, for $i \in [p]$. The optimal multimarginal transport plan between μ_1, \dots, μ_p for the problem (8) is given by the Gaussian measure*

$$\mathcal{N} \left(\begin{bmatrix} m_1 \\ m_2 \\ \vdots \\ m_p \end{bmatrix}, \begin{bmatrix} \Sigma_1 & C_{12} & \cdots & C_{1p} \\ C_{12}^\top & \Sigma_2 & \cdots & C_{2p} \\ \vdots & \vdots & \ddots & \vdots \\ C_{1p}^\top & C_{2p}^\top & \cdots & \Sigma_p \end{bmatrix} \right),$$

where $\{C_{ij}\}_{i \neq j} \subset \mathbb{R}^{d \times d}$ solve the semidefinite program

$$\begin{aligned} \max_{\{C_{ij}\}} \quad & \sum_{i=1}^p \sum_{j=i+1}^p \text{tr}(C_{ij}) \\ \text{s.t.} \quad & \Sigma := \begin{bmatrix} \Sigma_1 & C_{12} & \cdots & C_{1p} \\ C_{12}^\top & \Sigma_2 & \cdots & C_{2p} \\ \vdots & \vdots & \ddots & \vdots \\ C_{1p}^\top & C_{2p}^\top & \cdots & \Sigma_p \end{bmatrix} \succeq 0. \end{aligned}$$

The solution of this problem exists, is unique, and satisfies $\text{rank}(\Sigma) = d$.

Theorem 4.2 implies that the optimal multimarginal Gaussian plan—a probability measure over \mathbb{R}^{dp} —is obtained by pushing the isotropic Gaussian measure in \mathbb{R}^d through p linear functions $\ell_1, \dots, \ell_p : \mathbb{R}^d \rightarrow \mathbb{R}^d$. Namely, the optimal plan is $(\ell_1, \dots, \ell_p)_\# \mathcal{N}(0, I) \in \Pi(\mu_1, \dots, \mu_p)$.

To prove **Theorem 4.2**, we expand the cost function and argue that the optimal coupling can be chosen to be jointly Gaussian since the optimization problem only depends on the centered covariance of π . The last part of the result follows from a theorem of [Gangbo and Świąch \(1998\)](#), which shows that the optimal coupling is supported on a deterministic map, implying that the optimal coupling is supported on a d -dimensional submanifold of \mathbb{R}^{dp} . Finally, the proof of **Theorem 4.2** concludes by arguing that this submanifold must actually be a linear subspace of \mathbb{R}^{dp} since the conditional expectation of one coordinate of a Gaussian given another is affine.

Example 4.1 (Visualization of multimarginal OT). We can further provide insight into the structure of the optimal multimarginal coupling through a representative example. Suppose that $p = 3$ and that $\mu_i = \mathcal{N}(0, \Sigma_i)$, $i \in [3]$, are centered Gaussians. We can solve the semidefinite program in **Theorem 4.2** using a standard interior-point method ([Diamond and Boyd, 2016](#)) to obtain the optimal coupling π between μ_1, μ_2, μ_3 . Although π is a measure on \mathbb{R}^6 , **Theorem 4.2** implies that it is

supported on a 2-dimensional linear subspace of \mathbb{R}^6 . Therefore, we can visualize the nondegenerate part of π by projecting onto this 2-dimensional subspace. We display such an example in Figure 4.

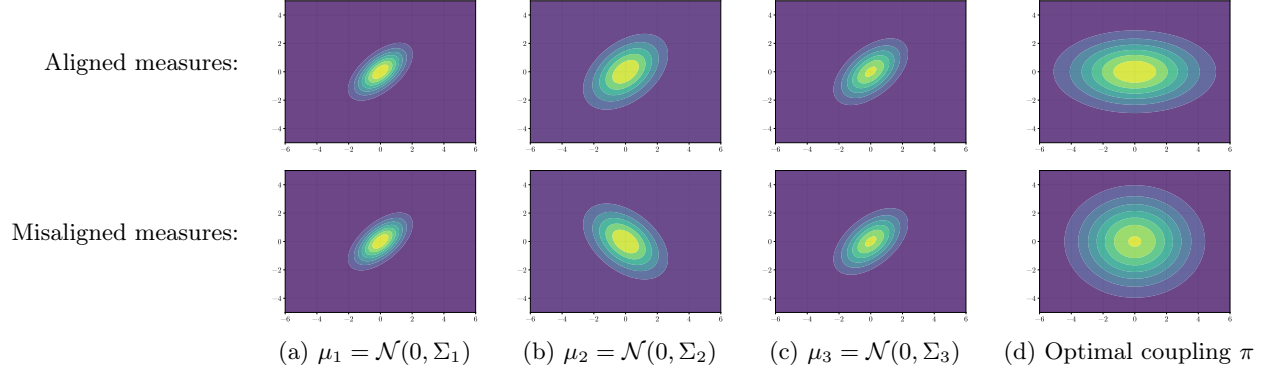


Figure 4: *Comparison of multimarginal OT between two sets of Gaussian distributions. Top row: multimarginal OT between three misaligned Gaussians. Bottom row: multimarginal OT between three aligned Gaussians.*

From Figure 4, we see that the optimal coupling π can afford to be less spread out when the input measures are more aligned, so that even a “flatter” two-dimensional covariance structure can be orthogonally transformed in \mathbb{R}^6 to have the correct marginals. This is in contrast to the top row in Figure 4, where the input measures are not aligned, which forced the optimal multimarginal coupling to be more spread out.

4.3 An Efficient Burer-Monteiro Algorithm for Multimarginal OT

A natural question following Theorem 4.2 is whether the rank deficiency of the solution can help design faster algorithms for solving the semidefinite program. We answer this question in the affirmative, by proposing one such approach based on the Burer-Monteiro factorization (Burer and Monteiro, 2003). Fix $k \leq dp$ and consider the optimization problem

$$\begin{aligned} \inf_{U=(U_1^\top, \dots, U_p^\top)^\top \in \mathbb{R}^{dp \times k}} & - \sum_{i=1}^p \sum_{j=i+1}^p \text{tr}(U_i U_j^\top) \\ \text{s.t. } & U_i U_i^\top = \Sigma_i \quad \text{for } i \in [p] \end{aligned}$$

and let $\mathcal{M} := \{U = (U_1^\top, \dots, U_p^\top)^\top \in \mathbb{R}^{dp \times k} : U_i U_i^\top = \Sigma_i \text{ for } i \in [p]\}$ denote the search space, which is a smooth and compact Riemannian submanifold of $\mathbb{R}^{dp \times k}$. By Corollary 8 of Boumal et al. (2016), if $U = (U_1^\top, \dots, U_p^\top)^\top \in \mathbb{R}^{dp \times k}$ is a rank-deficient second-order stationary point of the above problem (as defined in Appendix E), then $C_{ij} = U_i U_j^\top$ is a *global* optimizer of the problem in Theorem 4.2.

In particular, so long as we can find a rank-deficient second-order stationary point of the above problem, we can solve the multimarginal OT problem between μ_1, \dots, μ_p .

While for general semidefinite programs one can only guarantee the existence of a second-order stationary point U with rank strictly less than $k \propto d\sqrt{p}$ (Boumal et al., 2016), in our setting, thanks to Theorem 4.2 we can always guarantee the existence of such a point by setting $k = d + 1$. This phenomenon is unusual for general semidefinite programs, and relies on the specific structure of our problem. The multimarginal solution can then be used to obtain the Gaussian barycenter, as per Proposition 2.1. We summarize these results in the following theorem.

Theorem 4.3 (Burer-Monteiro for multimarginal OT). *Let $\mu_i = \mathcal{N}(m_i, \Sigma_i)$ be Gaussian measures on \mathbb{R}^d with $\Sigma_i \succ 0$ for $i \in [p]$. Suppose $U \in \mathbb{R}^{dp \times (d+1)}$ is any second-order stationary point of*

$$\begin{aligned} \inf_{U=(U_1^\top, \dots, U_p^\top)^\top \in \mathbb{R}^{dp \times (d+1)}} & - \sum_{i=1}^p \sum_{j=i+1}^p \text{tr}(U_i U_j^\top) \\ \text{s.t. } & U_i U_i^\top = \Sigma_i \quad \text{for } i \in [p]. \end{aligned}$$

Then, the Gaussian measure $\mathcal{N}((m_1^\top, \dots, m_p^\top)^\top, UU^\top)$ solves the multimarginal OT problem between μ_1, \dots, μ_p . Further, define $U_{\mu_i} := U_i$ for $i \in [p]$. If $\rho \in \mathcal{P}(\mathcal{P}_2(\mathbb{R}^d))$ has $\text{supp}(\rho) = \{\mu_1, \dots, \mu_p\}$, then the ρ -weighted 2-Wasserstein barycenter is

$$\bar{\mu} := \mathcal{N}\left(\int m_\nu d\rho(\nu), \left(\int U_\nu d\rho(\nu)\right)\left(\int U_\nu d\rho(\nu)\right)^\top\right).$$

Though the original semidefinite program in Theorem 4.2 has $d^2 p^2$ optimization variables, the optimization problem in Theorem 4.3 has only $(d+1)dp$ variables, which is a significant reduction when p is large. Now, finding second-order stationary points of the problem in Theorem 4.3 can be done using standard optimization techniques. For example, second-order manifold optimization methods such as trust-region schemes almost always converge to second-order stationary points under mild conditions (e.g., see Theorem 6.20 of Boumal (2023)). Therefore, Theorem 4.3 immediately yields a method to efficiently compute the multimarginal OT between a large number of Gaussian measures. Furthermore, Theorem 4.3 provides an alternative method for computing the 2-Wasserstein barycenter between Gaussian measures (equivalently, finding barycenters between positive definite matrices in the Bures-Wasserstein geometry).

5 Experiments

In this section, we illustrate the practical utility of our results in several applications. First, we propose the IGW distance as a new principled metric for comparing the representational similarity of large language models (LLMs). We also include numerical experiments which illustrate the effectiveness of our Burer-Monteiro approach to solving Gaussian multimarginal OT. All code for our experiments can be found at the following GitHub repository:

<https://github.com/sanjitdp/gaussian-gw>

5.1 IGW Metric for Representation Similarity of Language Models

Consider a set $\mathcal{S} \subseteq \mathcal{V}^k$ of sentences (over a vocabulary \mathcal{V} and context length k) and let $\varphi : \mathcal{V}^k \rightarrow \mathbb{R}^d$ represent the forward pass of a black-box LLM from the input to an internal representation space. Comparing the representations $\varphi(\mathcal{S})$ of different LLMs φ has seen notable recent interest (Morcos et al., 2018; Kornblith et al., 2019; Csiszárík et al., 2021). Existing approaches first embed the dataset into \mathbb{R}^d using each model and then compare the resulting point clouds using a similarity metric. The typical setting involves comparing a large model φ to many smaller distillation models $\varphi_1, \dots, \varphi_p$ on a dataset $\mathcal{D} = \{d_1, \dots, d_n\} \subseteq \mathcal{S}$, to find the small model whose representations best align with those of φ . This problem can be viewed as a question of comparing the distributions $\frac{1}{n} \sum_{i=1}^n \delta_{\varphi(d_i)}$ and $\frac{1}{n} \sum_{i=1}^n \delta_{\varphi_j(d_i)}$, for $j \in [p]$.

5.1.1 Existing and Proposed Similarity Metrics

A common choice of similarity metric is the centered kernel alignment (CKA) introduced by Kornblith et al. (2019). Assuming that $(X_i, Y_i) \sim \pi$ are i.i.d. samples from some joint distribution $\pi \in \mathcal{P}_2(\mathbb{R}^{d_1} \times \mathbb{R}^{d_2})$, the empirical *centered kernel alignment* (CKA) between X and Y is

$$\text{CKA}(X, Y) := \frac{\|Y^\top X\|_F^2}{\|X^\top X\|_F \|Y^\top Y\|_F}.$$

In our setting, X and Y are taken as the embeddings of the dataset \mathcal{D} under two different models. However, the CKA metric was designed as a normalized version of $\|Y^\top X\|_F^2$, which measures the *statistical correlation* between two random variables. In particular, even if the CKA is 1, it is not necessarily true that one set of embeddings can be orthogonally transformed into the other one; hence, pairwise cosine similarities may not be preserved and the learned representations of the two models may be different. For the same reason, any metric to compare learned representations that

	$H = 128$	$H = 256$	$H = 512$	$H = 768$
$L = 2$	4.4	9.7	22.8	39.2
$L = 4$	4.8	11.3	29.1	53.4
$L = 6$	5.2	12.8	35.4	67.5
$L = 8$	5.6	14.4	41.7	81.7
$L = 10$	6.0	16.0	48.0	95.9
$L = 12$	6.4	17.6	54.3	110.1

Table 1: Number of parameters of the **bert** model distillations of [Turc et al. \(2019\)](#) (in millions), as a function of the number of transformer layers L and hidden embedding dimension H . The teacher model **bert-base-uncased** has $L = 12$ and $H = 768$, with 110.1 million parameters.

is translation-invariant, such as the commonly-used CCA family of metrics ([Morcos et al., 2018](#)), cannot compare text embedding distributions well.

To resolve these issues, we propose using the IGW distance as a principled method to compare the representational similarity of LLMs. The IGW distance is invariant to orthogonal transformations, so it respects the relative geometry of the distributions. When the IGW distance between two measures is zero, they must be separated by an orthogonal transformation, meaning that pairwise cosine similarities are all preserved. Furthermore, the IGW distance is compatible for the task of comparing distillations of LLMs as it can also handle distributions in different dimensions.

5.1.2 Gaussian Modeling Assumption and Verification

To employ our framework, we model text embedding distributions as Gaussian, which is a common practice in machine learning; see [Mroueh \(2019\)](#) and [Lv et al. \(2024\)](#) for instances closely related to our work, among many others.

To justify this modeling assumption, we first verify that the empirical distributions of text embeddings from LLMs on common datasets can be indeed approximated by Gaussians. For reference, we consider the **bert-base-uncased** teacher model and 23 of its distilled variants, described in [Turc et al. \(2019\)](#). The distillations are trained using a variety of numbers of transformer layers $L \in \{2, 4, 6, 8, 10, 12\}$, and hidden embedding dimensions $H \in \{128, 256, 512, 768\}$. We display the number of parameters, in millions, of each model in [Table 1](#).

We consider datasets of 1000 samples each from: (i) the **amazon_polarity** dataset ([Muennighoff et al., 2022](#)), which contains Amazon reviews, and (ii) the **ag_news** dataset ([Zhang et al., 2015](#)), which contains news articles from over 2000 different sources. First, we see that the learned representations of the models are approximately Gaussian. In [Figure 5](#), we plot the first two principal

components of the embeddings of the **bert-base-uncased** model on both datasets, along with a Gaussian fit using the empirical mean and covariance of the embeddings. Note that computing the 2-Wasserstein distance between the full high-dimensional distributions is statistically difficult due to the limited number of samples. However, the 2-Wasserstein distance between the projection of the embeddings onto their first two principal components and the associated Gaussian measure is 0.458 for **amazon_polarity** and 0.655 for **ag_news**; the fact that these are small implies that the embedding distributions are approximately close to Gaussian.

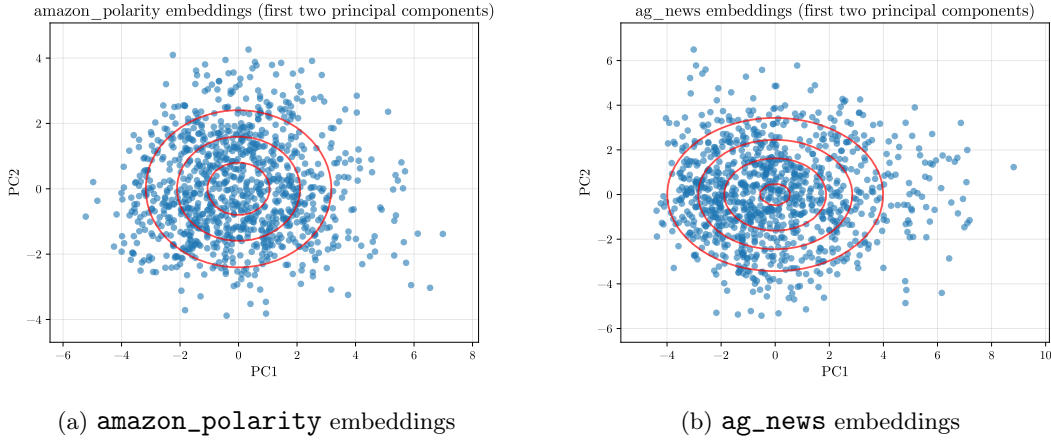


Figure 5: *First two principal components of the embeddings produced by the **bert-base-uncased** model on the (a) **amazon_polarity** and (b) **ag_news** datasets (blue), along with contour lines from a Gaussian fit (red). The embeddings are approximately Gaussian.*

5.1.3 LLM Representation Comparison via IGW

We now turn to compute the IGW distances between the **bert-base-uncased** teacher model and its 23 distillations from [Turc et al. \(2019\)](#). To employ our results for Gaussian IGW, we fit a Gaussian to the embeddings of each model on both datasets. For the Gaussian parameter estimation, we add a regularization of $10^{-6} I$ to the covariance for numerical stability. Then, we compute the analytic upper and lower bounds on the IGW distance from [Theorem 3.2](#). Furthermore, we tighten the upper bound by numerically optimizing over the Stiefel manifold $\text{St}(d, d)$ using RGD ([Absil et al., 2008](#)) to solve the optimization problem in [Theorem 3.1](#). Recall from [Corollary 3.1](#) that the validity of the upper bound does not rely on the Gaussianity assumption.

We run RGD with a simple adaptive step size for 50 iterations or until the norm of the Riemannian gradient is less than 10^{-2} . Estimating each IGW distance, including upper and lower bounds,

takes under 1 second on our MacBook using an M1 Pro chip. We show the results in Figure 6.

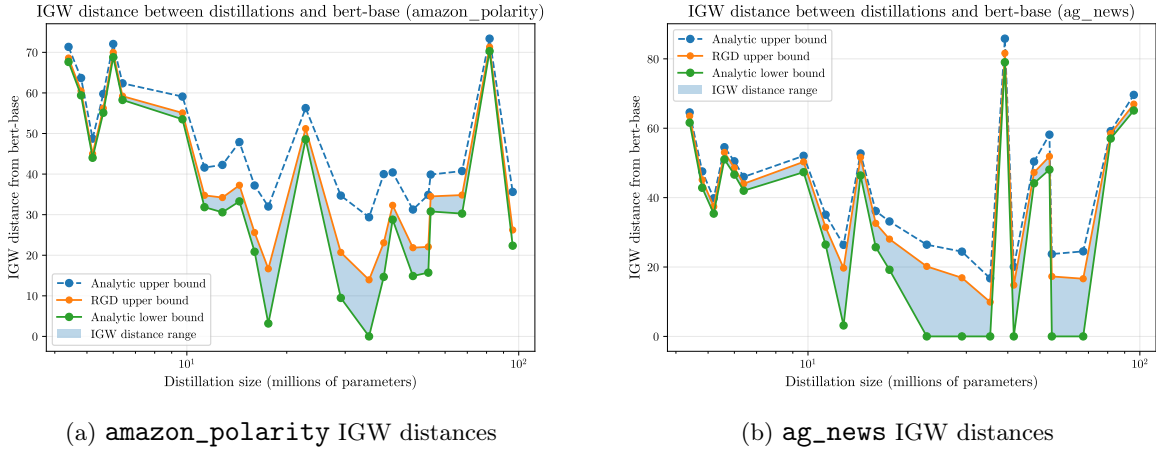


Figure 6: *Upper and lower bounds on the IGW distance between the `bert-base-uncased` model and its distillations on the (a) `amazon_polarity` and (b) `ag_news` datasets. The analytic upper bound is tightened by numerically optimizing over the Stiefel manifold. We see that some of the smaller distillations preserve the embedding distribution almost as well as the larger ones. The resulting upper and lower bounds are usually tight enough to reasonably compare the models.*

Although we motivated the IGW distance as a principled alternative to CKA, we observe that the two metrics are correlated in practice. In Figure 7, we plot the CKA between the `bert-base-uncased` model and its distillations on both datasets, and compare it to the upper bound on the IGW distance obtained by RGD. We see that the two metrics are generally negatively correlated, suggesting that the IGW distance will work well in settings where CKA is currently used.

Note that the problem of representational similarity is a question about preservation of the *overall embedding distributions*, and not about the performance of the models on a specific task. For instance, it may be possible that a distillation of an LLM performs well on a classification task, but the learned representations are very different from those of the original model. Therefore, we do not compare the IGW distance to task-specific metrics such as accuracy or F1 score; this is analogous to the original treatment of CKA in Kornblith et al. (2019).

5.2 Heterogeneous User Clustering

Clustering based on text data, e.g., users of a social media platform based on their text posts, is ubiquitous across applications. A common approach is to embed the text into a Euclidean space using an LLM, and then represent each user as the mean embedding of their posts (sometimes

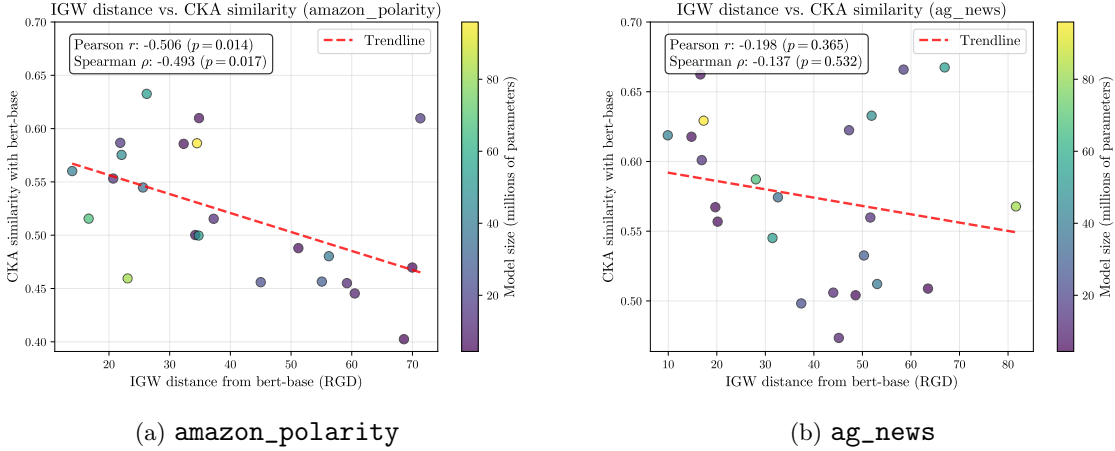


Figure 7: *CKA between the `bert-base-uncased` model and its distillations on the (a) `amazon_polarity` and (b) `ag_news` datasets, compared to the upper bound on the IGW distance obtained by RGD. The two metrics are generally negatively correlated, suggesting that the IGW distance will work well as a theoretically grounded alternative to CKA.*

called mean-pooling) (Chen et al., 2018); see also (Nguyen et al., 2025) for a recent application of mean-pooling to 3-D object image embedding. Once each user has been mean-pooled into a single embedding, one can cluster them using standard Euclidean algorithms, such as k -means or density-based methods. While popular in practice, such approaches forfeit valuable distributional information (e.g., the user’s embedding covariance).

Next, we show that the IGW distance enables a novel clustering algorithm that can leverage such information. We consider a synthetic user clustering task based on their text posts and simulate differences in interests across users by drawing posts from three different categories. We construct a population of 120 users arranged into three interest groups: science, news, and entertainment. Each group contains 40 users, and each user is represented by 400 non-overlapping posts drawn uniformly from `scientific_papers/arxiv` (Cohan et al., 2018), `ag_news` (Zhang et al., 2015), and `imdb` (Maas et al., 2011), respectively.

We embed each user’s posts using the `all-MiniLM-L6-v2` sentence embedding model from Hugging Face (Wang et al., 2020). Discarding the mean information, we then model each user as $\mathcal{N}(0, \Sigma_i)$, where Σ_i is the empirical covariance matrix of their embeddings. This modeling choice is made to highlight the utility of IGW-based clustering compared to mean-pooling, as the latter cannot leverage covariance information. We compute the IGW distance between each pair of users using Theorem 3.1, and then perform k -means++ clustering (Arthur and Vassilvitskii, 2006) on

the resulting distance matrix using the barycenter formula in [Proposition 3.3](#) to compute cluster centers. The results are shown in [Figure 8](#). We see that the IGW distance is almost able to recover the original clusters using only covariance information, suggesting that current approaches based on mean-pooling are missing valuable information contained in the full distribution of each user’s embeddings. One simple way to incorporate covariance information into existing methods is to add (a positive multiple of) the IGW distance between the centered Gaussians to the mean-pooled distances between users before clustering.

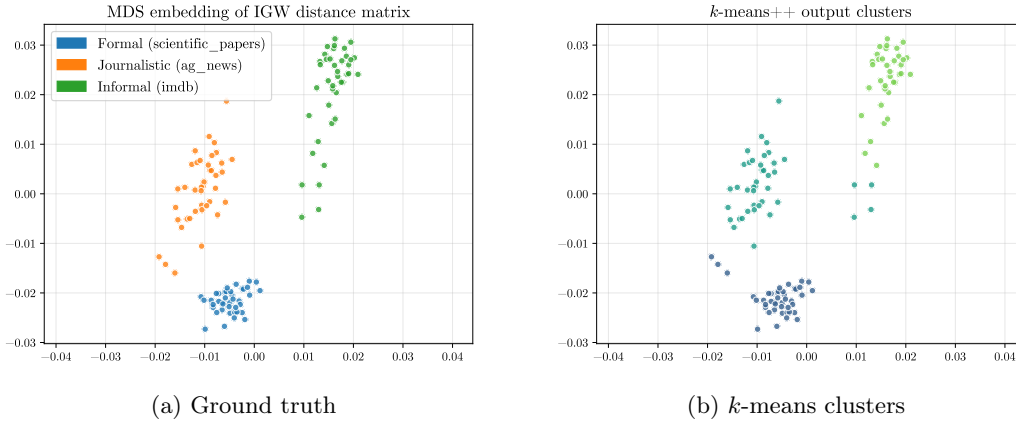


Figure 8: (a) 2-D multi-dimensional scaling (MDS) embedding of the IGW distance matrix between users, colored by their ground truth interests. (b) k -means++ clustering of the IGW distance matrix, using the barycenter formula in [Proposition 3.3](#) to compute cluster centers. The IGW distance is able to almost recover the original clusters, using only covariance information.

The IGW clustering algorithm is flexible in allowing for input measures over Euclidean space of different dimensions. To illustrate this, we repeat the above experiment, but embed each user via one of two LLMs with different embedding dimensions based on a random (fair) coin flip: either `all-MiniLM-L6-v2` ($d = 384$) as before, or `all-mpnet-base-v2` ($d = 768$), which was introduced in [Song et al. \(2020\)](#). Such a situation could arise in practice if some users were using a previous version of an application with an older embedding model. While the different embedding dimensions render mean-pooling inapplicable in this setting, the IGW distance still provides a viable path to clustering. We again model each user as a centered Gaussian with covariance equal to the empirical covariance of their text embeddings. [Figure 9](#) shows the 2-D MDS embedding of the IGW distance matrix (with colors showing the embedding models for each user), the ground truth interests of the users, and the result of the k -means++ algorithm applied to the IGW distance. Again, the obtained

clusters match the original ones almost perfectly.

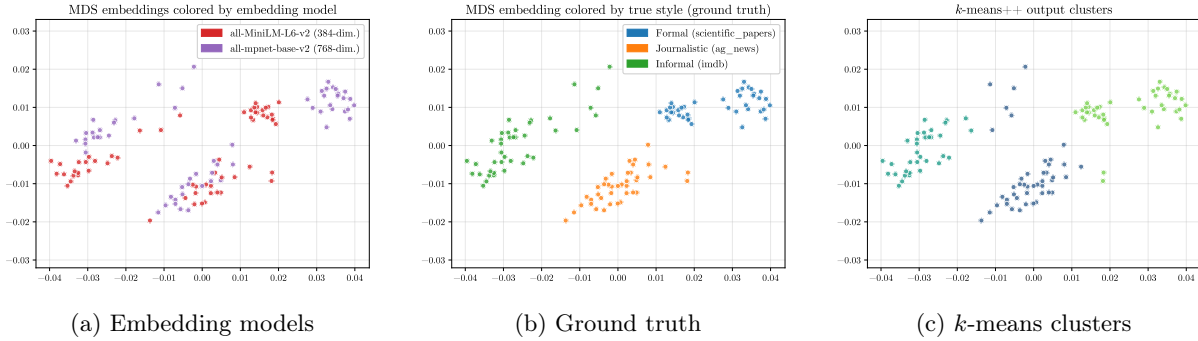


Figure 9: (a) 2-D MDS embedding of the IGW distance matrix between users, colored by the embedding model used for each user. (b) The same MDS embedding, colored by the ground truth interests of each user. (c) k -means++ clustering of the IGW distance matrix between heterogeneous users, using the barycenter formula in Proposition 3.3 to compute cluster centers. The IGW distance is able to almost recover the original clusters, even only using heterogeneous covariance information.

5.3 Efficient Computation of Multimarginal OT

In this section, we show that the Burer-Monteiro approach of Theorem 4.3 can be used to solve the multimarginal OT problem between Gaussian measures efficiently. We consider p Gaussian measures $\mu_i = \mathcal{N}(0, \Sigma_i)$ on \mathbb{R}^3 , where the Σ_i are generated by sampling $A_i \in \mathbb{R}^{3 \times 3}$ with i.i.d. standard normal entries and setting $\Sigma_i = A_i A_i^\top + 0.1 I$. We solve the semidefinite program in Theorem 4.2 using the Burer-Monteiro approach of Theorem 4.3 with $k = 11$, using Riemannian trust-region methods (Absil et al., 2008) to find second-order stationary points. We compare our results to the solution of the semidefinite program using the `cvxpy` package (Diamond and Boyd, 2016), which uses interior-point methods to solve semidefinite programs. All experiments were run on a MacBook with an M1 Pro processor. We display the results in Figure 10a and Figure 10b. To contextualize the speedup and improvement in numerical stability of the Burer-Monteiro approach as compared to the SDP approach, we plot the number of optimization variables in Figure 10c.

Usually, one computes the 2-Wasserstein barycenter by solving the non-linear matrix equation in (5) via fixed-point iteration. Alternatively, we can compute it by solving the semidefinite program in Theorem 4.2 and taking a weighted average of the coordinates in the resulting coupling; see Proposition 2.1. Even so, we observe in simulations that the fixed-point iteration is faster and more numerically stable for computing the barycenter than solving the full multimarginal problem.

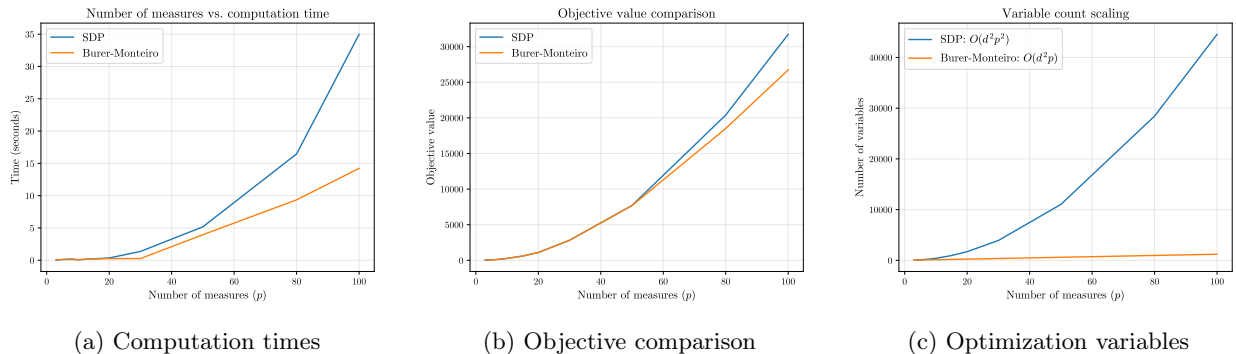


Figure 10: Comparison of the Burer-Monteiro and interior-point approaches for solving the multimarginal OT problem between p Gaussian measures on \mathbb{R}^3 : (a) computation times, (b) objective values, (c) number of optimization variables. The Burer-Monteiro approach is significantly faster than interior-point methods for large p , and the objective values are more numerically stable; note that the Burer-Monteiro approach is able to obtain a slightly better objective value when p is large. The Burer-Monteiro approach has significantly fewer optimization variables ($O(d^2 p)$ compared to $O(d^2 p^2)$) when p is large, explaining its speedup and improved numerical stability.

6 Conclusion

This work studies quadratic OT and IGW alignment problems between Gaussian measures in several settings. We show that the IGW distance between uncentered Gaussians can be written as an optimization problem over unitary transformations and use this formulation to characterize the Gaussian IGW distance and barycenter in closed-form. We also derive upper and lower bounds on the IGW distance between uncentered Gaussians which are separated only by a Cauchy-Schwarz gap. For the OT setting, we show that the multimarginal problem with pairwise quadratic cost between Gaussian measures is equivalent to a rank-deficient semidefinite program. The rank-deficiency constraint enables employing Burer-Monteiro factorization for efficient computation of the multimarginal OT cost and optimal coupling. Building on our theory, we explore applications to tasks concerning LLM representation comparisons and clustering of text embeddings. The resulting methods are shown to be flexible, cheap to compute, and perform well across all examined scenarios.

Finally, we discuss potential future directions for this work. Although [Theorem 3.1](#) formulates the IGW distance between Gaussian measures as a nonconvex Riemannian optimization problem, it would be interesting to analytically study whether Riemannian gradient flow always converges to a *global* minimum for this problem. Empirically, we observe that when pairwise IGW distances

between many Gaussian measures are computed via RGD, the resulting distances satisfy the triangle inequality. Furthermore, the distances obtained from RGD agree in experiments with all of our known closed-form cases, suggesting that RGD may indeed be converging to a global minimum. Another interesting direction is to study the intrinsic Riemannian geometry induced by the GBW distance on the space of nondegenerate covariance operators.

References

- Kantorovich, L. V. (1942). On the translocation of masses. *Dokl. Akad. Nauk. USSR (NS)*, 37, 199–201.
- Bauer, H. (1958). Minimalstellen von funktionen und extremalpunkte. *Archiv der Mathematik*, 9(4), 389–393.
- Desoer, C. A., & Whalen, B. H. (1963). A note on pseudoinverses. *Journal of the Society for Industrial and Applied Mathematics*, 11(2), 442–447.
- Baker, C. R. (1973). Joint measures and cross-covariance operators. *Transactions of the American Mathematical Society*, 186, 273–289.
- Givens, C. R., & Shortt, R. M. (1984). A class of Wasserstein metrics for probability distributions. *Michigan Mathematical Journal*, 31(2), 231–240.
- Knott, M., & Smith, C. S. (1984). On the optimal mapping of distributions. *Journal of Optimization Theory and Applications*, 43, 39–49.
- Gelbrich, M. (1990). On a formula for the L^2 Wasserstein metric between measures on Euclidean and Hilbert spaces. *Mathematische Nachrichten*, 147(1), 185–203.
- Brenier, Y. (1991). Polar factorization and monotone rearrangement of vector-valued functions. *Communications on pure and applied mathematics*, 44(4), 375–417.
- Grigorieff, R. D. (1991). A Note on von Neumann’s Trace Inequality. *Mathematische Nachrichten*, 151(1), 327–328.
- Bogachev, V. I. (1998). *Gaussian measures*. American Mathematical Society.
- Gangbo, W., & Świąch, A. (1998). Optimal maps for the multidimensional Monge-Kantorovich problem. *Communications on Pure and Applied Mathematics*, 51(1), 23–45.
- Burer, S., & Monteiro, R. D. (2003). A nonlinear programming algorithm for solving semidefinite programs via low-rank factorization. *Mathematical programming*, 95(2), 329–357.
- Villani, C. (2003). *Topics in optimal transportation* (Vol. 58). American Mathematical Society.

- Boyd, S. P., & Vandenberghe, L. (2004). *Convex optimization*. Cambridge University Press.
- Simon, B. (2005). *Trace ideals and their applications*. American Mathematical Society.
- Arthur, D., & Vassilvitskii, S. (2006). *K-means++: The advantages of careful seeding* (tech. rep.). Stanford.
- Loiola, E. M., De Abreu, N. M. M., Boaventura-Netto, P. O., Hahn, P., & Querido, T. (2007). A survey for the quadratic assignment problem. *European Journal of Operational Research*, 176(2), 657–690.
- Absil, P.-A., Mahony, R., & Sepulchre, R. (2008). *Optimization algorithms on matrix manifolds*. Princeton University Press.
- Agueh, M., & Carlier, G. (2011). Barycenters in the Wasserstein space. *SIAM Journal on Mathematical Analysis*, 43(2), 904–924.
- Maas, A. L., Daly, R. E., Pham, P. T., Huang, D., Ng, A. Y., & Potts, C. (2011). Learning word vectors for sentiment analysis, 142–150.
- Mémoli, F. (2011). Gromov-Wasserstein distances and the metric approach to object matching. *Foundations of Computational Mathematics*, 11, 417–487.
- Rabin, J., Peyré, G., Delon, J., & Marc, B. (2011). Wasserstein barycenter and its application to texture mixing. *International Conference on Scale Space and Variational Methods in Computer Vision*, 435–446.
- Cuturi, M. (2013). Sinkhorn distances: Lightspeed computation of optimal transport. *Advances in Neural Information Processing Systems*, 26.
- Pass, B. (2015). Multi-marginal optimal transport: Theory and applications. *ESAIM: Mathematical Modelling and Numerical Analysis*, 49(6), 1771–1790.
- Zhang, X., Zhao, J., & LeCun, Y. (2015). Character-level convolutional networks for text classification. *Advances in Neural Information Processing Systems*, 28.
- Boumal, N., Voroninski, V., & Bandeira, A. (2016). The non-convex Burer-Monteiro approach works on smooth semidefinite programs. *Advances in Neural Information Processing Systems*, 29.
- Diamond, S., & Boyd, S. (2016). CVXPY: A Python-embedded modeling language for convex optimization. *Journal of Machine Learning Research*, 17(83), 1–5.
- Arjovsky, M., Chintala, S., & Bottou, L. (2017). Wasserstein generative adversarial networks. *International Conference on Machine Learning*, 214–223.

- Courty, N., Flamary, R., Habrard, A., & Rakotomamonjy, A. (2017). Joint distribution optimal transportation for domain adaptation. *Advances in Neural Information Processing Systems*, 30.
- Ho, N., Nguyen, X., Yurochkin, M., Bui, H. H., Huynh, V., & Phung, D. (2017). Multilevel clustering via Wasserstein means. *International Conference on Machine Learning*, 1501–1509.
- Alvarez-Melis, D., & Jaakkola, T. S. (2018). Gromov-Wasserstein alignment of word embedding spaces. *arXiv preprint arXiv:1809.00013*.
- Chen, Q., Ling, Z.-H., & Zhu, X. (2018). Enhancing sentence embedding with generalized pooling. *arXiv preprint arXiv:1806.09828*.
- Cohan, A., Dernoncourt, F., Kim, D. S., Bui, T., Kim, S., Chang, W., & Goharian, N. (2018). A discourse-aware attention model for abstractive summarization of long documents. *Proceedings of the 2018 Conference of the North American Chapter of the Association for Computational Linguistics: Human Language Technologies, Volume 2 (Short Papers)*, 615–621.
- Mi, L., Zhang, W., Gu, X., & Wang, Y. (2018). Variational Wasserstein clustering. *Proceedings of the European Conference on Computer Vision (ECCV)*, 322–337.
- Morcos, A., Raghu, M., & Bengio, S. (2018). Insights on representational similarity in neural networks with canonical correlation. *Advances in Neural Information Processing Systems*, 31.
- Bunne, C., Alvarez-Melis, D., Krause, A., & Jegelka, S. (2019). Learning generative models across incomparable spaces. *International Conference on Machine Learning*, 851–861.
- Dukler, Y., Li, W., Lin, A., & Montúfar, G. (2019). Wasserstein of Wasserstein loss for learning generative models. *International Conference on Machine Learning*, 1716–1725.
- Kolouri, S., Nadjahi, K., Simsekli, U., Badeau, R., & Rohde, G. (2019). Generalized sliced Wasserstein distances. *Advances in Neural Information Processing Systems*, 32.
- Kornblith, S., Norouzi, M., Lee, H., & Hinton, G. (2019). Similarity of neural network representations revisited, 3519–3529.
- Lee, C.-Y., Batra, T., Baig, M. H., & Ulbricht, D. (2019). Sliced Wasserstein discrepancy for unsupervised domain adaptation. *Proceedings of the IEEE/CVF Conference on Computer Vision and Pattern Recognition (CVPR)*, 10285–10295.
- Mroueh, Y. (2019). Wasserstein style transfer. *arXiv preprint arXiv:1905.12828*.
- Peyré, G., & Cuturi, M. (2019). Computational optimal transport: With applications to data science. *Foundations and Trends in Machine Learning*, 11(5-6), 355–607.

- Turc, I., Chang, M.-W., Lee, K., & Toutanova, K. (2019). Well-read students learn better: On the importance of pre-training compact models. *arXiv preprint arXiv:1908.08962*.
- Vayer, T., Flamary, R., Courty, N., Tavenard, R., & Chapel, L. (2019). Sliced Gromov-Wasserstein. *Advances in Neural Information Processing Systems*, 32.
- Xu, H., Luo, D., Zha, H., & Duke, L. C. (2019). Gromov-Wasserstein learning for graph matching and node embedding. *International Conference on Machine Learning*, 6932–6941.
- Makkuva, A., Taghvaei, A., Oh, S., & Lee, J. (2020). Optimal transport mapping via input convex neural networks. *International Conference on Machine Learning*, 6672–6681.
- Song, K., Tan, X., Qin, T., Lu, J., & Liu, T.-Y. (2020). MPNet: masked and permuted pre-training for language understanding. *Advances in Neural Information Processing Systems*, 33, 16857–16867.
- Vayer, T. (2020). A contribution to optimal transport on incomparable spaces. *arXiv preprint arXiv:2011.04447*.
- Wang, W., Wei, F., Dong, L., Bao, H., Yang, N., & Zhou, M. (2020). MiniLM: deep self-attention distillation for task-agnostic compression of pre-trained transformers. *Advances in Neural Information Processing Systems*, 33, 5776–5788.
- Csiszár, A., Kőrösi-Szabó, P., Matszangosz, A., Papp, G., & Varga, D. (2021). Similarity and matching of neural network representations. *Advances in Neural Information Processing Systems*, 34, 5656–5668.
- Daniels, M., Maunu, T., & Hand, P. (2021). Score-based generative neural networks for large-scale optimal transport. *Advances in neural information processing systems*, 34, 12955–12965.
- Brogat-Motte, L., Flamary, R., Brouard, C., Rousu, J., & d’Alché-Buc, F. (2022). Learning to predict graphs with fused Gromov-Wasserstein barycenters. *International Conference on Machine Learning*, 2321–2335.
- Demetci, P., Santorella, R., Sandstede, B., Noble, W. S., & Singh, R. (2022). SCOT: single-cell multi-omics alignment with optimal transport. *Journal of Computational Biology*, 29(1), 3–18.
- Kwon, D., Fan, Y., & Lee, K. (2022). Score-based generative modeling secretly minimizes the Wasserstein distance. *Advances in Neural Information Processing Systems*, 35, 20205–20217.
- Le, K., Le, D. Q., Nguyen, H., Do, D., Pham, T., & Ho, N. (2022). Entropic Gromov-Wasserstein between Gaussian distributions. *International Conference on Machine Learning*, 12164–12203.

- Muennighoff, N., Tazi, N., Magne, L., & Reimers, N. (2022). MTEB: Massive Text Embedding Benchmark. *arXiv preprint arXiv:2210.07316*.
- Nietert, S., Goldfeld, Z., Sadhu, R., & Kato, K. (2022). Statistical, robustness, and computational guarantees for sliced Wasserstein distances. *Advances in Neural Information Processing Systems*, 35, 28179–28193.
- Salmona, A., Delon, J., & Desolneux, A. (2022). Gromov-Wasserstein distances between Gaussian distributions. *Journal of Applied Probability*, 59(4), 1178–1198.
- Beier, F., Beinert, R., & Steidl, G. (2023). Multi-marginal Gromov-Wasserstein transport and barycentres. *Information and Inference: A Journal of the IMA*, 12(4), 2753–2781.
- Boumal, N. (2023). *An introduction to optimization on smooth manifolds*. Cambridge University Press.
- Cooper, D. (2023). *Applications of the Bures-Wasserstein Distance in Linear Metric Learning* [Doctoral dissertation, Open Access Te Herenga Waka-Victoria University of Wellington].
- Han, A., Mishra, B., Jawanpuria, P., & Gao, J. (2023). Learning with symmetric positive definite matrices via generalized Bures-Wasserstein geometry. *International Conference on Geometric Science of Information*, 405–415.
- Klein, D., Uscidda, T., Theis, F., & Cuturi, M. (2023). Entropic (Gromov) Wasserstein Flow Matching with GENOT. *arXiv preprint arXiv:2310.09254*, 9.
- Koehl, P., Delarue, M., & Orland, H. (2023). Computing the Gromov-Wasserstein distance between two surface meshes using optimal transport. *Algorithms*, 16(3), 131.
- Bikchentaev, A. M., Kittaneh, F., Moslehian, M. S., & Seo, Y. (2024). *Trace Inequalities: For Matrices and Hilbert Space Operators*. Springer.
- Haviv, D., Pooladian, A.-A., Pe’er, D., & Amos, B. (2024). Wasserstein flow matching: Generative modeling over families of distributions. *arXiv preprint arXiv:2411.00698*.
- Kawakita, G., Zeleznikow-Johnston, A., Tsuchiya, N., & Oizumi, M. (2024). Gromov-Wasserstein unsupervised alignment reveals structural correspondences between the color similarity structures of humans and large language models. *Scientific Reports*, 14(1), 15917.
- Klein, D., Uscidda, T., Theis, F., & Cuturi, M. (2024). GENOT: Entropic (Gromov) Wasserstein flow matching with applications to single-cell genomics. *Advances in Neural Information Processing Systems*, 37, 103897–103944.
- Lv, J., Yang, H., & Li, P. (2024). Wasserstein distance rivals Kullback-Leibler divergence for knowledge distillation. *Advances in Neural Information Processing Systems*, 37, 65445–65475.

- Mokrov, P., Korotin, A., Kolesov, A., Gushchin, N., & Burnaev, E. (2024). Energy-guided entropic neural optimal transport. *International Conference on Learning Representations*.
- Rioux, G., Goldfeld, Z., & Kato, K. (2024). Entropic Gromov-Wasserstein distances: Stability and Algorithms. *Journal of Machine Learning Research*, 25(363), 1–52.
- Wang, T., & Goldfeld, Z. (2024). Neural estimation of entropic optimal transport. *IEEE International Symposium on Information Theory*, 2116–2121.
- Zhang, Z., Goldfeld, Z., Mroueh, Y., & Sriperumbudur, B. K. (2024). Gromov-Wasserstein distances: entropic regularization, duality and sample complexity. *The Annals of Statistics*, 52(4), 1616–1645.
- Chambers, E. W., & Meng, G. (2025). A Stable and Theoretically Grounded Gromov-Wasserstein Distance for Reeb Graph Comparison using Persistence Images. *arXiv preprint arXiv:2507.01171*.
- Dumont, T., Lacombe, T., & Vialard, F.-X. (2025). On the existence of Monge maps for the Gromov-Wasserstein problem. *Foundations of Computational Mathematics*, 25(2), 463–510.
- Naumann, P., Kauffmann, J., & Montavon, G. (2025). Wasserstein distances made explainable: Insights into dataset shifts and transport phenomena. *arXiv preprint arXiv:2505.06123*.
- Nguyen, P., Verdoja, F., & Kyrki, V. (2025). REACT: Real-time Efficient Attribute Clustering and Transfer for Updatable 3D Scene Graph. *arXiv preprint arXiv:2503.03412*.
- Zhang, Z., Goldfeld, Z., Greenewald, K., Mroueh, Y., & Sriperumbudur, B. K. (2025). Gradient Flows and Riemannian Structure in the Gromov-Wasserstein Geometry. *Foundations of Computational Mathematics*.

A Proofs of Main Results

In this section, we collect proofs of our main results.

A.1 Proof of Theorem 3.1

We begin with a technical lemma that will be useful in the proof of Theorem 3.1.

Lemma A.1 (Cyclic property of trace). *Suppose that $\mu_i \in \mathcal{P}_2(\mathcal{H})$ for $i \in [2]$ and that $\pi \in \Pi(\mu_1, \mu_2)$. Then, if $((X_1, X_2), (X'_1, X'_2)) \sim \pi \otimes \pi$, we have*

$$\mathbb{E}[\langle X_1, X'_1 \rangle \langle X_2, X'_2 \rangle] = \text{tr}((\Sigma_\pi^\times)^* \Sigma_\pi^\times).$$

Proof. The proof of this lemma is relatively standard and follows that of the usual cyclic property of trace in a Hilbert space, so we omit it here (e.g., see [Simon, 2005](#)). \square

Proof of Theorem 3.1. To find the IGW distance, we minimize over couplings $\pi \in \Pi(\mu_1, \mu_2)$. Define $\bar{\mu}_i = (\cdot - m_i)_\# \mu_i$ for $i \in [2]$. Then, it is equivalent to optimize over centered couplings $\bar{\pi} = ((\cdot + m_1), (\cdot + m_2))_\# \pi \in \Pi(\bar{\mu}_1, \bar{\mu}_2)$, which immediately yield couplings $\pi \in \Pi(\mu_1, \mu_2)$. By orthogonal invariance of the IGW distance ([Zhang et al., 2025](#)), if we define $\tilde{\mu}_i := (Q_i^*)_\# \bar{\mu}_i$ for $i \in [2]$, then $\text{IGW}(\tilde{\mu}_1, \tilde{\mu}_2) = \text{IGW}(\bar{\mu}_1, \bar{\mu}_2)$. Also, any coupling achieves the same IGW cost under orthogonal transformations of either marginal, so letting $\tilde{\pi}$ denote the optimal coupling for IGW between $\tilde{\mu}_1$ and $\tilde{\mu}_2$, the optimal coupling between $\bar{\mu}_1$ and $\bar{\mu}_2$ will be $\bar{\pi} = (Q_1, Q_2)_\# \tilde{\pi}$.

Note that now $\tilde{\mu}_i = \mathcal{N}(0, \Lambda_i)$ for $i \in [2]$, and we may assume w.l.o.g. that $\text{range}(\Lambda_2) \subseteq \text{range}(\Lambda_1)$. Defining $\tilde{m}_i = Q_i^* m_i$ for $i \in [2]$, we rewrite the objective function as

$$\begin{aligned} & \int (\langle x_1 + \tilde{m}_1, x'_1 + \tilde{m}_1 \rangle - \langle x_2 + \tilde{m}_2, x'_2 + \tilde{m}_2 \rangle)^2 d(\tilde{\pi} \times \tilde{\pi})(x_1, x_2, x'_1, x'_2) \\ &= \underbrace{\left(\int \langle x_1 + \tilde{m}_1, x'_1 + \tilde{m}_1 \rangle^2 d(\tilde{\mu}_1 \times \tilde{\mu}_1)(x_1, x'_1) \right)}_{I_1} + \underbrace{\left(\int \langle x_2 + \tilde{m}_2, x'_2 + \tilde{m}_2 \rangle^2 d(\tilde{\mu}_2 \times \tilde{\mu}_2)(x_2, x'_2) \right)}_{I_2} \\ & \quad - 2 \underbrace{\int \langle x_1 + \tilde{m}_1, x'_1 + \tilde{m}_1 \rangle \langle x_2 + \tilde{m}_2, x'_2 + \tilde{m}_2 \rangle d(\tilde{\pi} \times \tilde{\pi})(x_1, x_2, x'_1, x'_2)}_{I_3}. \end{aligned}$$

Letting $(X_1, X'_1) \sim \tilde{\mu}_1 \times \tilde{\mu}_1$, we can compute the first integral explicitly as

$$\begin{aligned} I_1 &= \int \langle x_1 + \tilde{m}_1, x'_1 + \tilde{m}_1 \rangle^2 d(\tilde{\mu}_1 \times \tilde{\mu}_1)(x_1, x'_1) \\ &= \mathbb{E}[\langle X_1 + \tilde{m}_1, X'_1 + \tilde{m}_1 \rangle^2] \\ &= \mathbb{E}[\langle X_1, X'_1 \rangle^2] + \mathbb{E}[\langle X_1, \tilde{m}_1 \rangle^2] + \mathbb{E}[\langle X'_1, \tilde{m}_1 \rangle^2] + \|\tilde{m}_1\|^4 \\ & \quad + 2 \mathbb{E}[\langle X_1, \tilde{m}_1 \rangle \langle X'_1, \tilde{m}_1 \rangle] + 2 \|\tilde{m}_1\|^2 \mathbb{E}[\langle X_1, X'_1 \rangle]. \end{aligned}$$

The last two terms vanish because $\tilde{\mu}_1$ is centered and $\mathbb{E}[\langle X_1, X'_1 \rangle] = \mathbb{E}[\mathbb{E}[\langle X_1, X'_1 \rangle \mid X'_1]] = 0$ by the tower property of conditional expectation. By definition, the second and third terms are equal to $\langle \tilde{m}_1, \Lambda_1 \tilde{m}_1 \rangle$. Using [Lemma A.1](#) with $\pi = \tilde{\mu}_1 \times \tilde{\mu}_1$, the first term is $\mathbb{E}[\langle X_1, X'_1 \rangle^2] = \text{tr}(\Lambda_1^2)$. Putting the pieces together, we have shown that

$$I_1 = \text{tr}(\Lambda_1^2) + 2\langle \tilde{m}_1, \Lambda_1 \tilde{m}_1 \rangle + \|\tilde{m}_1\|^4.$$

Analogously, the second integral is

$$I_2 = \text{tr}(\Lambda_2^2) + 2\langle \tilde{m}_2, \Lambda_2 \tilde{m}_2 \rangle + \|\tilde{m}_2\|^4.$$

Finally, let C denote the cross-covariance operator between $\tilde{\mu}_1$ and $\tilde{\mu}_2$ with respect to $\tilde{\pi}$. Drawing $((X_1, X_2), (X'_1, X'_2)) \sim \tilde{\pi} \times \tilde{\pi}$, we write

$$\begin{aligned}
I_3 &= \int \langle x_1 + \tilde{m}_1, x'_1 + \tilde{m}_1 \rangle \langle x_2 + \tilde{m}_2, x'_2 + \tilde{m}_2 \rangle d(\tilde{\pi} \times \tilde{\pi})(x_1, x_2, x'_1, x'_2) \\
&= \mathbb{E}[\langle X_1 + \tilde{m}_1, X'_1 + \tilde{m}_1 \rangle \langle X_2 + \tilde{m}_2, X'_2 + \tilde{m}_2 \rangle] \\
&= \mathbb{E}[\langle X_1, X_2 \rangle \langle X'_1, X'_2 \rangle] + \mathbb{E}[\langle X_1, \tilde{m}_1 \rangle \langle X_2, X'_2 \rangle] + \mathbb{E}[\langle X_1, X'_1 \rangle \langle X_2, \tilde{m}_2 \rangle] \\
&\quad + \mathbb{E}[\langle X_1, X'_1 \rangle \langle \tilde{m}_2, X'_2 + \tilde{m}_2 \rangle] + \mathbb{E}[\langle \tilde{m}_1, X'_1 + \tilde{m}_1 \rangle \langle X_2, X'_2 \rangle] \\
&\quad + \mathbb{E}[\langle X_1, \tilde{m}_1 \rangle \langle X_2, \tilde{m}_2 \rangle] + \mathbb{E}[\langle \tilde{m}_1, X'_1 \rangle \langle \tilde{m}_2, X'_2 \rangle] + \|\tilde{m}_1\|^2 \|\tilde{m}_2\|^2.
\end{aligned}$$

The second term vanishes because

$$\begin{aligned}
\mathbb{E}[\langle X_1, \tilde{m}_1 \rangle \langle X_2, X'_2 \rangle] &= \mathbb{E}[\mathbb{E}[\langle X_1, \tilde{m}_1 \rangle \langle X_2, X'_2 \rangle \mid X_1, X_2]] \\
&= \mathbb{E}[\langle X_1, \tilde{m}_1 \rangle \mathbb{E}[\langle X_2, X'_2 \rangle \mid X_1, X_2]] = 0
\end{aligned}$$

by the tower property of conditional expectation; the third, fourth, and fifth terms vanish by a similar argument. The sixth and seventh terms are $\mathbb{E}[\langle X_1, \tilde{m}_1 \rangle \langle X_2, \tilde{m}_2 \rangle] = \langle \tilde{m}_1, \Sigma_{\tilde{\pi}}^{\times} \tilde{m}_2 \rangle$. By [Lemma A.1](#), the first term is $\mathbb{E}[\langle X_1, X_2 \rangle \langle X'_1, X'_2 \rangle] = \text{tr}((\Sigma_{\tilde{\pi}}^{\times})^* \Sigma_{\tilde{\pi}}^{\times})$. Using this, we conclude that

$$I_3 = \text{tr}((\Sigma_{\tilde{\pi}}^{\times})^* \Sigma_{\tilde{\pi}}^{\times}) + 2\langle \tilde{m}_1, \Sigma_{\tilde{\pi}}^{\times} \tilde{m}_2 \rangle + \|\tilde{m}_1\|^2 \|\tilde{m}_2\|^2.$$

Now, our optimization problem becomes

$$\begin{aligned}
&\inf_{\|\Sigma_{\tilde{\pi}}^{\times}\|_{\text{op}} < \infty} \text{tr}(\Lambda_1^2) + \text{tr}(\Lambda_2^2) + 2\langle \tilde{m}_1, \Lambda_1 \tilde{m}_1 \rangle + 2\langle \tilde{m}_2, \Lambda_2 \tilde{m}_2 \rangle + (\|\tilde{m}_1\|^2 - \|\tilde{m}_2\|^2)^2 \\
&\quad - 2(\text{tr}((\Sigma_{\tilde{\pi}}^{\times})^* \Sigma_{\tilde{\pi}}^{\times}) + 2\langle \tilde{m}_1, \Sigma_{\tilde{\pi}}^{\times} \tilde{m}_2 \rangle) \\
&\text{s.t. } \Sigma_{\tilde{\pi}}^{\times} \text{ is the cross-covariance operator of some coupling } \tilde{\pi} \in \Pi(\tilde{\mu}_1, \tilde{\mu}_2).
\end{aligned}$$

Since the objective is only affected by the covariance operator of the coupling $\tilde{\pi}$, we may assume without loss of generality that $\tilde{\pi}$ is a Gaussian coupling ([Bogachev, 1998](#)). We can therefore replace the constraint with

$$\begin{bmatrix} \Lambda_1 & \Sigma_{\tilde{\pi}}^{\times} \\ (\Sigma_{\tilde{\pi}}^{\times})^* & \Lambda_2 \end{bmatrix} \succeq 0,$$

where the block matrix is to be interpreted as a block operator on the Hilbert space $\mathcal{H} \oplus \mathcal{H}$ ([Bikchentaev et al., 2024](#), Section 1.6).

Because $\Lambda_i \succeq 0$ for $i \in [2]$, the constraints are equivalent to the set of Schur complement constraints $\Lambda_1 - \Sigma_{\tilde{\pi}}^{\times} \Lambda_2^{\dagger} (\Sigma_{\tilde{\pi}}^{\times})^* \succeq 0$ and $(I - \Lambda_2 \Lambda_2^{\dagger}) \Sigma_{\tilde{\pi}}^{\times} = 0$ (this is an immediate consequence of

Theorem 1.6.1 of [Bikchentaev et al. \(2024\)](#) and the discussion in Appendix A.5.5 of [Boyd and Vandenberghe \(2004\)](#)). The constraint $(I - \Lambda_2 \Lambda_2^\dagger) \Sigma_\pi^\times = 0$ forces the range of Σ_π^\times to be contained in the range of Λ_2 . Since we assumed $\text{range}(\Lambda_2) \subseteq \text{range}(\Lambda_1)$ and the objective is invariant to the action of Σ_π^\times on $\text{range}(\Lambda_1)^\perp$, we can write $\Sigma_\pi^\times = \Lambda_2^{1/2} C \Lambda_1^{1/2}$ for some bounded linear operator C . Now, $P = \Lambda_2^{1/2} \Lambda_2^\dagger \Lambda_2^{1/2}$ is an orthogonal projection onto the range of Λ_2 , so we have

$$\Lambda_1 - C \Lambda_2^\dagger C^* \succeq 0 \iff \Lambda_1 - \Lambda_1^{1/2} C (\Lambda_2^{1/2} \Lambda_2^\dagger \Lambda_2^{1/2}) C^* \Lambda_1^{1/2} \succeq 0 \iff I - C P C^* \succeq 0$$

and $\text{tr}(C^* C) = \text{tr}(C \Lambda_1 C^* \Lambda_2)$ by the cyclic property of trace. Replacing $CP \mapsto C$ (because the objective is invariant to the action of C on $\text{range}(\Lambda_1)^\perp$) and using that $\Lambda_2^{1/2}$ is self-adjoint, we can rewrite the optimization equivalently as

$$\begin{aligned} \sup_{\|C\|_{\text{op}} < \infty} \quad & \text{tr}(C \Lambda_1 C^* \Lambda_2) + 2 \langle C \Lambda_1^{1/2} \tilde{m}_1, \Lambda_2^{1/2} \tilde{m}_2 \rangle \\ \text{s.t.} \quad & C C^* \preceq I. \end{aligned}$$

Next, we show that the objective is continuous in C with respect to the weak-* topology on the space of bounded linear operators on \mathcal{H} . We rewrite the objective as $\|\Lambda_2^{1/2} C \Lambda_1^{1/2}\|_{\text{HS}}^2 + 2 \langle C \Lambda_1^{1/2} \tilde{m}_1, \Lambda_2^{1/2} \tilde{m}_2 \rangle$, and we compute

$$\begin{aligned} \|\Lambda_2^{1/2} C \Lambda_1^{1/2}\|_{\text{HS}}^2 &= \sum_{i=1}^{\infty} \sum_{j=1}^{\infty} \langle v_i, \Lambda_2^{1/2} C \Lambda_1^{1/2} v_j \rangle^2 \\ &= \sum_{i=1}^{\infty} \sum_{j=1}^{\infty} \langle \Lambda_2^{1/2} v_i, C \Lambda_1^{1/2} v_j \rangle^2 \\ &= \sum_{i=1}^{\infty} \sum_{j=1}^{\infty} \lambda_i(\Lambda_2) \lambda_j(\Lambda_1) \langle v_i, C v_j \rangle^2. \end{aligned}$$

Suppose that $C_n \rightarrow C$ converges in the weak-* topology, so that $\text{tr}(A C_n) \rightarrow \text{tr}(A C)$ for all trace-class operators A . Then, we have that $\langle v_i, C_n v_j \rangle = \text{tr}((v_j \otimes v_i) C_n) \rightarrow \text{tr}((v_j \otimes v_i) C) = \langle v_i, C v_j \rangle$ for all $i, j \in \mathbb{N}$ since $v_j \otimes v_i$ is trace-class. By the uniform boundedness principle, the C_n are uniformly bounded in operator norm because they converge in the weak-* topology. Therefore, the dominated convergence theorem implies that $\|\Lambda_2^{1/2} C_n \Lambda_1^{1/2}\|_{\text{HS}}^2 \rightarrow \|\Lambda_2^{1/2} C \Lambda_1^{1/2}\|_{\text{HS}}^2$. Obviously, the map $A \mapsto \|A\|_{\text{HS}}^2$ is continuous in the Hilbert-Schmidt norm, so the first term is continuous in the weak-* topology as it is the composition of continuous maps. The second term is continuous in the weak-* topology because $\langle C \Lambda_1^{1/2} \tilde{m}_1, \Lambda_2^{1/2} \tilde{m}_2 \rangle = \text{tr}(((\Lambda_2^{1/2} \tilde{m}_2) \otimes (\Lambda_1^{1/2} \tilde{m}_1)) C)$ and $(\Lambda_2^{1/2} \tilde{m}_2) \otimes (\Lambda_1^{1/2} \tilde{m}_1)$ is trace-class.

The objective is convex; the first term is an affine map followed by a squared norm and the second term is affine. By the Banach-Alaoglu theorem, the set of linear operators C with $\|C\|_{\text{op}} \leq 1$ is compact in the weak-* topology. Finally, because we are maximizing a convex upper semi-continuous function over a compact convex set, the supremum is attained at an extreme point of the feasible set by Bauer's maximum principle ([Bauer, 1958](#)), which means that we may replace the constraint $CC^* \preceq I$ with the constraint $CC^* = I$.

Finally, it's easy to see that $CC^* = I$ if and only if C is unitary. The forward direction is immediate; for the reverse direction, note that for all $x, y \in \mathcal{H}$,

$$\langle x, y \rangle = \langle C^*x, C^*y \rangle = \langle x, CC^*y \rangle \implies \langle x, (CC^* - I)y \rangle = 0.$$

Therefore, we get

$$\begin{aligned} 0 &= \langle x + y, (CC^* - I)(x + y) \rangle \\ &= \langle x, (CC^* - I)x \rangle + \langle y, (CC^* - I)y \rangle + 2\langle x, (CC^* - I)y \rangle \\ &= 2\langle x, (CC^* - I)y \rangle, \end{aligned}$$

and choosing $x = (CC^* - I)y$ gives the result since y was arbitrary. The optimal coupling between μ_1 and μ_2 follows from inverting the transformations at the start of the proof, and the formula for the IGW distance follows by plugging in the optimal value of C . \square

A.2 Proof of [Theorem 3.2](#)

By [Theorem 3.1](#), we have that

$$\text{IGW}(\mu_1, \mu_2)^2 = \text{tr}(\Lambda_1^2) + \text{tr}(\Lambda_2^2) + 2\langle \tilde{m}_1, \Lambda_1 \tilde{m}_1 \rangle + 2\langle \tilde{m}_2, \Lambda_2 \tilde{m}_2 \rangle + (\|\tilde{m}_1\|^2 - \|\tilde{m}_2\|^2)^2 - 2\gamma(\mu_1, \mu_2),$$

where $\gamma(\mu_1, \mu_2)$ is the optimal value of

$$\begin{aligned} \inf_{C \in \mathcal{L}(\mathcal{H})} \quad & \text{tr}(\Lambda_1 C^* \Lambda_2 C) + \langle C \Lambda_1^{1/2} \tilde{m}_1, \Lambda_2^{1/2} \tilde{m}_2 \rangle \\ \text{s.t.} \quad & C \in \mathcal{U}(\mathcal{H}). \end{aligned}$$

By the von Neumann trace inequality (which applies to Hilbert-Schmidt operators in a separable Hilbert space by Remark 1 of [Grigorieff \(1991\)](#)), we have

$$\text{tr}(\Lambda_1 C^* \Lambda_2 C) \leq \sum_{k=1}^{\infty} \lambda_k(\Lambda_1) \lambda_k(C^* \Lambda_2 C) = \sum_{k=1}^{\infty} \lambda_k(\Lambda_1) \lambda_k(\Lambda_2),$$

and this upper bound is achieved by the feasible choice $C = I$. By the Cauchy-Schwarz inequality and using that C is unitary, we have

$$\langle \Sigma_1^{1/2} \tilde{m}_1, C \Sigma_2^{1/2} \tilde{m}_2 \rangle \leq \|\Sigma_1^{1/2} \tilde{m}_1\| \|C \Sigma_2^{1/2} \tilde{m}_2\| \leq \|C\|_{\text{op}} \|\Sigma_1^{1/2} \tilde{m}_1\| \|\Sigma_2^{1/2} \tilde{m}_2\| = \|\Sigma_1^{1/2} \tilde{m}_1\| \|\Sigma_2^{1/2} \tilde{m}_2\|,$$

and this upper bound is achieved by the feasible choice

$$C = \frac{(\Sigma_2^{1/2} \tilde{m}_1) \otimes (\Sigma_2^{1/2} \tilde{m}_2)}{\|\Sigma_1^{1/2} \tilde{m}_1\| \|\Sigma_2^{1/2} \tilde{m}_2\|}.$$

Since each term in the optimization problem defining $\gamma(\mu_1, \mu_2)$ is individually bounded above (subject to the constraint), we immediately obtain the lower bound on $\text{IGW}(\mu_1, \mu_2)^2$. The upper bound follows easily from choosing $C = I$ in the objective.

A.3 Proof of Corollary 3.1

Until we reached the optimization problem

$$\begin{aligned} \inf_{\|C\|_{\text{op}} < \infty} \quad & \text{tr}(\Lambda_1^2) + \text{tr}(\Lambda_2^2) + 2\langle \tilde{m}_1, \Lambda_1 \tilde{m}_1 \rangle + 2\langle \tilde{m}_2, \Lambda_2 \tilde{m}_2 \rangle + (\|\tilde{m}_1\|^2 - \|\tilde{m}_2\|^2)^2 \\ & - 2(\text{tr}((\Sigma_{\tilde{\pi}}^{\times})^* \Sigma_{\tilde{\pi}}^{\times}) + 2\langle \tilde{m}_1, \Sigma_{\tilde{\pi}}^{\times} \tilde{m}_2 \rangle) \\ \text{s.t.} \quad & \Sigma_{\tilde{\pi}}^{\times} \text{ is the cross-covariance operator of some coupling } \tilde{\pi} \in \Pi(\tilde{\mu}_1, \tilde{\mu}_2) \end{aligned}$$

in the proof of Theorem 3.1, we did not use the Gaussianity assumption. Now, any valid coupling $\tilde{\pi} \in \Pi(\tilde{\mu}_1, \tilde{\mu}_2)$ must have a cross-covariance operator $\Sigma_{\tilde{\pi}}^{\times}$ satisfying

$$\begin{bmatrix} \Lambda_1 & \Sigma_{\tilde{\pi}}^{\times} \\ (\Sigma_{\tilde{\pi}}^{\times})^* & \Lambda_2 \end{bmatrix} \succeq 0,$$

so replacing the constraint with this necessary condition yields a relaxation of the original problem. Hence, the solution of the relaxed problem (which is exactly the problem solved in Theorem 3.1) is an upper bound on the IGW distance between μ_1 and μ_2 .

A.4 Proof of Corollary 3.2

Proof of (i) in Corollary 3.2. The upper and lower bounds of Theorem 3.2 match under the assumption that $\Lambda_1^{1/2} \tilde{m}_1 = \alpha \Lambda_2^{1/2} \tilde{m}_2$ for some $\alpha \geq 0$; this corresponds to the equality case of the Cauchy-Schwarz inequality. \square

Proof of (ii) in Corollary 3.2. This follows immediately from Theorem 3.1 since the only unitary operators on \mathbb{R} are ± 1 . \square

Proof of Proposition 3.3. Using (i) in Corollary 3.2 along with Tonelli's theorem, we have

$$\begin{aligned} \int \text{IGW}(\mu, \nu)^2 d\rho(\nu) &= \int \sum_{k=1}^{\infty} (\lambda_k(\Sigma_\mu) - \lambda_k(\Sigma_\nu))^2 d\rho(\nu) \\ &= \sum_{k=1}^{\infty} \int (\lambda_k(\Sigma_\mu) - \lambda_k(\Sigma_\nu))^2 d\rho(\nu). \end{aligned}$$

Hence, the optimization problem decomposes across the eigenvalues of Σ_μ , and is strictly convex in each $\lambda_k(\Sigma_\mu)$ for $k \in \mathbb{N}$, subject to the constraint that $\lambda_k(\Sigma_\mu) \geq 0$. Let $\bar{\lambda}_k := \int \lambda_k(\Sigma_\nu) d\rho(\nu)$ for $k \in \mathbb{N}$. Then, we can rewrite

$$\begin{aligned} &\int (\lambda_k(\Sigma_\mu) - \lambda_k(\Sigma_\nu))^2 d\rho(\nu) \\ &= \int ((\lambda_k(\Sigma_\mu) - \bar{\lambda}_k) - (\lambda_k(\Sigma_\nu) - \bar{\lambda}_k))^2 d\rho(\nu) \\ &= \int (\lambda_k(\Sigma_\nu) - \bar{\lambda}_k)^2 d\rho(\nu) - 2(\lambda_k(\Sigma_\mu) - \bar{\lambda}_k) \int (\lambda_k(\Sigma_\nu) - \bar{\lambda}_k) d\rho(\nu) + (\lambda_k(\Sigma_\mu) - \bar{\lambda}_k)^2. \end{aligned}$$

The integral in the second term vanishes by definition of $\bar{\lambda}_k$ and the first term is constant with respect to $\lambda_k(\Sigma_\mu)$, so the objective function is minimized when $\lambda_k(\Sigma_\mu) = \bar{\lambda}_k$; this choice is nonnegative and therefore feasible, yielding the result. \square

A.5 Proof of Theorem 4.1

Define the projection maps $\Pi_{ij}(x_1, \dots, x_p) := (x_i, x_j)$ for $1 \leq i < j \leq p$ and let $\pi \in \Pi(\mu_1, \dots, \mu_p)$. Defining $\pi_{ij} := (\Pi_{ij})_\# \pi$ and letting $C_{ij} := \Sigma_{\pi_{ij}}^\times$, we can use Lemma A.1 to rewrite the objective as

$$\begin{aligned} &\int \sum_{i=1}^p \sum_{j=i+1}^p (\langle x_i, x'_i \rangle - \langle x_j, x'_j \rangle)^2 d(\pi \otimes \pi)(x_1, \dots, x_p, x'_1, \dots, x'_p) \\ &= \sum_{i=1}^p \sum_{j=i+1}^p (\text{tr}(\Sigma_i^2) + \text{tr}(\Sigma_j^2) - 2 \text{tr}(C_{ij}^* C_{ij})). \end{aligned}$$

Since the only constraints are on the covariance of the coupling, we may assume that the coupling π is jointly Gaussian so that the multimarginal IGW problem reduces to the optimization problem

$$\begin{aligned} &\sup_{\|C_{ij}\|_{\text{op}} < \infty} \sum_{i=1}^p \sum_{j=i+1}^p \text{tr}(C_{ij}^* C_{ij}) \\ &\text{s.t. } \Sigma := \begin{bmatrix} \Sigma_1 & C_{12} & \cdots & C_{1p} \\ C_{12}^* & \Sigma_2 & \cdots & C_{2p} \\ \vdots & \vdots & \ddots & \vdots \\ C_{1p}^* & C_{2p}^* & \cdots & \Sigma_p \end{bmatrix} \succeq 0. \end{aligned}$$

Now, this constraint immediately implies that

$$\begin{bmatrix} \Sigma_i & C_{ij} \\ C_{ij}^* & \Sigma_j \end{bmatrix} \succeq 0$$

for $1 \leq i < j \leq p$. We know from the proof of (i) in [Corollary 3.2](#) that the solution of

$$\sup_{\|C_{ij}\|_{\text{op}} < \infty} \text{tr}(C_{ij}^* C_{ij}) \quad \text{s.t.} \quad \begin{bmatrix} \Sigma_i & C_{ij} \\ C_{ij}^* & \Sigma_j \end{bmatrix} \succeq 0$$

is $C_{ij} = Q_i \Lambda_i^{1/2} \Lambda_j^{1/2} Q_j^*$, so it will suffice to show that this choice is feasible for the original problem.

To see this, note that for all $x = (x_1, \dots, x_p) \in \oplus_{i=1}^p \mathcal{H}$, we have

$$\begin{aligned} \langle x, \Sigma x \rangle &= \left\langle (x_1, \dots, x_p), \left(\sum_{j=1}^p Q_1 \Lambda_1^{1/2} \Lambda_j^{1/2} Q_j^* x_j, \sum_{j=1}^p Q_2 \Lambda_2^{1/2} \Lambda_j^{1/2} Q_j^* x_j, \dots, \sum_{j=1}^p Q_p \Lambda_p^{1/2} \Lambda_j^{1/2} Q_j^* x_j \right) \right\rangle \\ &= \sum_{i=1}^p \left\langle x_i, Q_i \Lambda_i^{1/2} \sum_{j=1}^p \Lambda_j^{1/2} Q_j^* x_j \right\rangle = \left\langle \sum_{i=1}^p \Lambda_i^{1/2} Q_i^* x_i, \sum_{j=1}^p \Lambda_j^{1/2} Q_j^* x_j \right\rangle = \left\| \sum_{i=1}^p \Lambda_i^{1/2} Q_i^* x_i \right\|^2 \geq 0, \end{aligned}$$

which shows that $\Sigma \succeq 0$ and completes the proof.

A.6 Proof of [Theorem 4.2](#)

We begin by reducing to the case of centered measures. Fix a coupling $\pi \in \Pi(\mu_1, \dots, \mu_p)$, let $\tilde{\mu}_i = \mathcal{N}(0, \Sigma_i)$ for $i \in [p]$, and define $\tilde{\pi} \in \Pi(\tilde{\mu}_1, \dots, \tilde{\mu}_p)$ by $\tilde{\pi} = ((\cdot - m_1), \dots, (\cdot - m_p))_{\#} \pi$. Now, we can write

$$\begin{aligned} &\int \sum_{i=1}^p \sum_{j=i+1}^p \|x_i - x_j\|_2^2 d\pi(x_1, \dots, x_p) \\ &= \int \sum_{i=1}^p \sum_{j=i+1}^p \|x_i - x_j + m_i - m_j\|_2^2 d\tilde{\pi}(x_1, \dots, x_p) \\ &= \int \sum_{i=1}^p \sum_{j=i+1}^p (\|x_i - x_j\|_2^2 + 2\langle x_i - x_j, m_i - m_j \rangle + \|m_i - m_j\|_2^2) d\tilde{\pi}(x_1, \dots, x_p). \end{aligned}$$

The second term vanishes because $\tilde{\pi}$ is centered, so we have

$$\begin{aligned} &\int \sum_{i=1}^p \sum_{j=i+1}^p (\|x_i - x_j\|_2^2 + 2\langle x_i - x_j, m_i - m_j \rangle + \|m_i - m_j\|_2^2) d\tilde{\pi}(x_1, \dots, x_p) \\ &= \int \sum_{i=1}^p \sum_{j=i+1}^p \|x_i - x_j\|_2^2 d\tilde{\pi}(x_1, \dots, x_p) + \sum_{i=1}^p \sum_{j=i+1}^p \|m_i - m_j\|_2^2. \end{aligned}$$

Hence, it suffices to solve the multimarginal OT problem assuming that all of the input measures are centered. Now, let $\pi \in \Pi(\mu_1, \dots, \mu_p)$ be a coupling and define the projection maps $\Pi_{ij}(x_1, \dots, x_p) :=$

(x_i, x_j) for $1 \leq i < j \leq p$. Defining $\pi_{ij} := (\Pi_{ij})_{\#} \pi$ and letting $C_{ij} := \Sigma_{\pi_{ij}}^{\times}$, we can expand the objective as

$$\begin{aligned} \int \sum_{i=1}^p \sum_{j=i+1}^p \|x_i - x_j\|_2^2 d\pi(x_1, \dots, x_p) &= \int \sum_{i=1}^p \sum_{j=i+1}^p (\|x_i\|_2^2 - 2\langle x_i, x_j \rangle + \|x_j\|_2^2) d\pi(x_1, \dots, x_p) \\ &= \text{tr} \left(\sum_{i=1}^p \left((p-1) \Sigma_i - 2 \sum_{j=i+1}^p C_{ij} \right) \right). \end{aligned}$$

Since the input measures are Gaussian and the only constraints are on the covariance of the coupling, we may assume without loss of generality that π is a Gaussian coupling. Therefore, we can replace the optimization problem with the equivalent semidefinite program

$$\begin{aligned} \inf_{C_{ij} \in \mathbb{R}^{d \times d}} \quad & \text{tr} \left(\sum_{i=1}^p \left((p-1) \Sigma_i - 2 \sum_{j=i+1}^p C_{ij} \right) \right) \\ \text{s.t.} \quad & \begin{bmatrix} \Sigma_1 & C_{12} & \cdots & C_{1p} \\ C_{12}^{\top} & \Sigma_2 & \cdots & C_{2p} \\ \vdots & \vdots & \ddots & \vdots \\ C_{1p}^{\top} & C_{2p}^{\top} & \cdots & \Sigma_p \end{bmatrix} \succeq 0. \end{aligned}$$

Now, by Theorem 2.1 of [Gangbo and Świąch \(1998\)](#) (since $\mu_1, \dots, \mu_p \in \mathcal{P}_2(\mathbb{R}^d)$ and vanish on $(d-1)$ -rectifiable sets), there exist unique measurable maps $S_i : \mathbb{R}^d \rightarrow \mathbb{R}^d$ for $i \in \{2, \dots, p\}$ such that $\pi = (I, S_2, \dots, S_p)_{\#} \mu_1$ is the optimal coupling. However, we know since π is jointly Gaussian that $\mathbb{E}_{\pi}[X_i | X_1 = x] = C_{1i}^{\top} \Sigma_1^{-1} x = S_i(x)$ for Lebesgue-almost every $x \in \mathbb{R}$, where the conditional expectation exists and is unique Lebesgue-almost everywhere by the disintegration of measure. Hence, $S_i(x) = A_i x$ are linear Lebesgue-almost everywhere, and

$$C_{ij} = \mathbb{E}_{\pi}[X_i X_j^{\top}] = A_i \mathbb{E}_{\pi}[X_1 X_1^{\top}] A_j^{\top} = A_i \Sigma_1 A_j^{\top},$$

means that the optimal coupling has rank d .

B Recovering the Barycenter from Multimarginal IGW

In this section, we discuss the general connection between the multimarginal IGW problem and the IGW barycenter problem, which allows us to recover a special case of [Proposition 3.3](#). First, we define the projection maps

$$\Pi_{i,p+1}(x_1, \dots, x_p, x) := (x_i, x)$$

for $i \in [p]$ with $\Pi_{p+1}(x_1, \dots, x_p, x) := x$.

Lemma B.1. Fix $\rho \in \mathcal{P}(\mathcal{P}_2(\mathcal{H}))$ with $\text{supp}(\rho) = \{\mu_1, \dots, \mu_p\}$. Then, the solution of

$$\arg \min_{\mu \in \mathcal{P}_2(\mathcal{H})} \inf_{\pi \in \Pi(\mu_1, \dots, \mu_p, \mu)} \int \left(\int (\langle x_\nu, x'_\nu \rangle - \langle x, x' \rangle)^2 d\rho(\nu) \right) d(\pi \otimes \pi)(x_{\mu_1}, \dots, x_{\mu_p}, x, x'_{\mu_1}, \dots, x'_{\mu_p}, x')$$

is a ρ -weighted IGW barycenter. Conversely, if $\bar{\mu}$ is a ρ -weighted IGW barycenter, then we can construct $\pi \in \Pi(\mu_1, \dots, \mu_p, \bar{\mu})$ which solves the inner optimization problem and satisfies $(\Pi_{i,p+1})_\# \pi = \pi_i$, where π_i is the pairwise optimal coupling for the IGW problem between μ_i and $\bar{\mu}$.

Proof. Let $\rho_i := \rho(\mu_i)$ for $i \in [p]$. Suppose $\bar{\mu}$ solves the ρ -weighted IGW barycenter problem. Then, suppose that $\pi_i \in \Pi(\mu_i, \bar{\mu})$ is an optimal coupling for $\text{IGW}(\mu_i, \bar{\mu})$ for each $i \in [p]$. Then, by the gluing lemma (Lemma 7.6 of Villani (2003)), we can glue the couplings π_i together to obtain a coupling $\pi \in \Pi(\mu_1, \dots, \mu_p, \bar{\mu})$ such that $(\Pi_{i,p+1})_\# \pi = \pi_i$ for each $i \in [p]$. Then, we have

$$\begin{aligned} & \sum_{i=1}^p \rho_i \text{IGW}(\bar{\mu}, \mu_i)^2 \\ &= \sum_{i=1}^p \rho_i \int (\langle x_i, x'_i \rangle - \langle x, x' \rangle)^2 d(\pi_i \otimes \pi_i)(x_i, x'_i) \\ &= \int \sum_{i=1}^p \rho_i (\langle x_i, x'_i \rangle - \langle x, x' \rangle)^2 d(\pi \otimes \pi)(x_1, \dots, x_p, x, x'_1, \dots, x'_p, x') \\ &\geq \inf_{\mu \in \mathcal{P}_2(\mathcal{H})} \inf_{\pi \in \Pi(\mu_1, \dots, \mu_p, \mu)} \int \sum_{i=1}^p \rho_i (\langle x_i, x'_i \rangle - \langle x, x' \rangle)^2 d(\pi \otimes \pi)(x_1, \dots, x_p, x, x'_1, \dots, x'_p, x'). \end{aligned}$$

On the other hand, suppose that $\bar{\pi}$ solves the multimarginal problem in Lemma B.1. It's clear now that $\Pi_{i,p+1}(\bar{\pi})$ is a coupling in $\Pi(\mu_i, (\Pi_{p+1})_\# \bar{\pi})$ for each $i \in [p]$. In particular, we obtain

$$\begin{aligned} & \int \sum_{i=1}^p \rho_i (\langle x_i, x'_i \rangle - \langle x, x' \rangle)^2 d(\bar{\pi} \times \bar{\pi})(x_1, \dots, x_p, x, x'_1, \dots, x'_p, x') \\ &= \sum_{i=1}^p \rho_i \int (\langle x_i, x'_i \rangle - \langle x, x' \rangle)^2 d((\Pi_{i,p+1})_\# \bar{\pi} \times (\Pi_{i,p+1})_\# \bar{\pi})(x_i, x, x'_i, x') \\ &\geq \sum_{i=1}^p \rho_i \text{IGW}(\mu_i, (\Pi_{p+1})_\# \bar{\pi})^2 \\ &\geq \inf_{\mu \in \mathcal{P}_2(\mathcal{H})} \sum_{i=1}^p \rho_i \text{IGW}(\mu_i, \mu)^2. \end{aligned}$$

Now the result follows easily. □

Now, we can use Lemma B.1 to recover a special case of Proposition 3.3 with only finitely many centered Gaussian measures in the support of ρ .

Corollary B.1 (special case of [Proposition 3.3](#)). *Let \mathcal{H} be a separable Hilbert space. Suppose that $\rho \in \mathcal{P}(\mathcal{P}_2(\mathcal{H}))$ has finite support $\text{supp}(\rho) = \{\mu_1, \dots, \mu_p\} \subseteq \mathcal{G}_0(\mathcal{H})$. Fix any total orthonormal set $\{e_k\}_{k \in \mathbb{N}}$ of \mathcal{H} . Then, defining the covariance operator*

$$\Sigma := \sum_{k=1}^{\infty} \left(\int \lambda_k(\Sigma_\nu) d\rho(\nu) \right) e_k \otimes e_k,$$

the measure $\mathcal{N}(0, \Sigma)$ is a ρ -weighted IGW barycenter.

Proof. By [Lemma B.1](#) (and because the proof of [Theorem 4.1](#) is unaffected by the weights ρ_i), we can write the multimarginal formulation of the barycenter problem as

$$\arg \min_{\Sigma \succeq 0} \left\{ \sum_{i=1}^p \rho_i (\text{tr}(\Sigma_i^2) + \text{tr}(\Sigma^2) - 2 \text{tr}(\Sigma_i \Sigma)) \right\} = \arg \min_{\Sigma \succeq 0} \left\{ \sum_{k=1}^{\infty} \sum_{i=1}^p \rho_i (\lambda_k(\Sigma_i) - \lambda_k(\Sigma))^2 \right\}.$$

Now, the optimization problem decomposes across the eigenvalues of Σ and stationarity implies that $\lambda_k(\Sigma) = \sum_{i=1}^p \rho_i \lambda_k(\Sigma_i)$ for $k \in \mathbb{N}$, so the result follows. \square

C Optimal Transport Between Gaussian Measures

In this section, we discuss the 2-Wasserstein distance between Gaussian measures on \mathbb{R}^d and the resulting optimal coupling.

Theorem C.1. *If $\mu_1 = \mathcal{N}(m_1, \Sigma_1)$ and $\mu_2 = \mathcal{N}(m_2, \Sigma_2)$ are two Gaussian measures on \mathbb{R}^d with $\Sigma_1 \succ 0$ and $\Sigma_2 \succ 0$, then the OT map for the Kantorovich problem under the quadratic cost $c(x, y) = \|x - y\|_2^2$ is given by*

$$T(x) = \Sigma_1^{-1/2} (\Sigma_1^{1/2} \Sigma_2 \Sigma_1^{1/2})^{1/2} \Sigma_1^{-1/2} (x - m_1) + m_2,$$

which induces the Wasserstein distance

$$W_2(\mu_1, \mu_2) = \sqrt{\|m_1 - m_2\|_2^2 + \text{tr} \left(\Sigma_1 + \Sigma_2 - 2 (\Sigma_1^{1/2} \Sigma_2 \Sigma_1^{1/2})^{1/2} \right)}.$$

If $m_1 = m_2$, this is called the *Bures-Wasserstein distance* between symmetric positive definite matrices Σ_1 and Σ_2 . One option is to use Brenier's theorem to prove [Theorem C.1](#).

Proof (from [Knott and Smith \(1984\)](#)). We make the ansatz that the transport map $T(x) = Ax + b$ is affine. Furthermore, we pick $A \succeq 0$ so that T is the gradient of a convex function, which is required

by Brenier's theorem ([Theorem D.1](#)). There are no constraints on b , so we may assume w.l.o.g. that $m_1 = m_2$. Then, since we need

$$\Sigma_2 = \int (Ax)(Ax)^\top d\mu(x) = A\Sigma_1 A^\top,$$

this forces

$$\Sigma_1^{1/2} \Sigma_2 \Sigma_1^{1/2} = \Sigma_1^{1/2} (A\Sigma_1 A^\top) \Sigma_1^{1/2} = (\Sigma_1^{1/2} A \Sigma_1^{1/2})^2.$$

Solving for A yields the OT plan, and then some algebra gives the Wasserstein distance. \square

Another option is to give a more direct proof of [Theorem C.1](#) by expanding the cost function, without relying on Brenier's theorem.

Proof (modified from [Givens and Shortt \(1984\)](#)). We begin by reducing to the case of centered measures; this step works generally for the 2-Wasserstein distance and does not require the assumption that μ and ν are Gaussian. Define $\tilde{\mu}_1 = (\cdot - m_1)_\# \mu_1$ and $\tilde{\mu}_2 = (\cdot - m_2)_\# \mu_2$. Then, for any coupling $\pi \in \Pi(\mu_1, \mu_2)$, define $\tilde{\pi} = ((\cdot - m_1), (\cdot - m_2))_\# \pi$ so that

$$\begin{aligned} \int \|x - y\|_2^2 d\pi(x, y) &= \int \|(x + m_1) - (y + m_2)\|_2^2 d\tilde{\pi}(x, y) \\ &= \int \|x - y\|_2^2 d\tilde{\pi}(x, y) + \int \langle x - y, m_1 - m_2 \rangle d\tilde{\pi}(x, y) + \|m_1 - m_2\|_2^2. \end{aligned}$$

The middle term vanishes since $\tilde{\pi}$ is centered, so it is clear that

$$W_2(\mu, \nu)^2 = \inf_{\pi \in \Pi(\mu, \nu)} \int \|x - y\|_2^2 d\pi(x, y) = \inf_{\pi \in \Pi(\tilde{\mu}, \tilde{\nu})} \int \|x - y\|_2^2 d\pi(x, y) + \|m_1 - m_2\|_2^2$$

and it suffices to consider the case where $m_1 = m_2 = 0$. In this case, we obtain

$$\begin{aligned} W_2(\mu_1, \mu_2)^2 &= \inf_{\pi \in \Pi(\mu_1, \mu_2)} \int \|x - y\|_2^2 d\pi(x, y) \\ &= \int \|x\|_2^2 d\mu_1(x) + \int \|y\|_2^2 d\mu_2(y) - 2 \sup_{\pi \in \Pi(\mu_1, \mu_2)} \int \langle x, y \rangle d\pi(x, y). \end{aligned}$$

Since the optimization problem only depends on the covariance of the coupling π , we may assume without loss of generality that π is a Gaussian coupling. Letting $C := \mathbb{E}_{(X, Y) \sim \pi}[XY^\top]$, the 2-Wasserstein distance is therefore the optimal value of the following semidefinite program:

$$\begin{aligned} \inf_{\Sigma_\pi^\times \in \mathbb{R}^{d \times d}} \quad & \text{tr}(\Sigma_1 + \Sigma_2 - 2\Sigma_\pi^\times) \\ \text{s.t.} \quad & \begin{bmatrix} \Sigma_1 & \Sigma_\pi^\times \\ (\Sigma_\pi^\times)^\top & \Sigma_2 \end{bmatrix} \succeq 0. \end{aligned}$$

Because $\Sigma_2 \succ 0$, the constraint is equivalent to the Schur complement constraint $\Sigma_1 - \Sigma_\pi^\times \Sigma_2^{-1} (\Sigma_\pi^\times)^\top \succeq 0$. The Lagrangian for this problem is

$$\mathcal{L}(\Sigma_\pi^\times, \Lambda) = \text{tr}(\Sigma_1 + \Sigma_2 - 2\Sigma_\pi^\times) - \text{tr}(\Lambda(\Sigma_1 - \Sigma_\pi^\times \Sigma_2^{-1} (\Sigma_\pi^\times)^\top))$$

for $\Lambda \succeq 0$. Finally, we use the KKT conditions to characterize the solution. By stationarity, we have

$$D_{\Sigma_\pi^\times} \mathcal{L}(\Sigma_\pi^\times, \Lambda) = -2I + 2\Lambda \Sigma_\pi^\times \Sigma_2^{-1} = 0 \implies \Lambda \Sigma_\pi^\times = \Sigma_2.$$

Complementary slackness (together with stationarity) gives

$$\Lambda(\Sigma_1 - \Sigma_\pi^\times \Sigma_2^{-1} (\Sigma_\pi^\times)^\top) = 0 \implies \Lambda \Sigma_1 = \Lambda \Sigma_\pi^\times \Sigma_2^{-1} (\Sigma_\pi^\times)^\top \implies \Lambda \Sigma_1 = (\Sigma_\pi^\times)^\top \implies \Sigma_\pi^\times = \Sigma_1 \Lambda.$$

Plugging this back in to the stationarity condition, we find that $\Lambda \Sigma_1 \Lambda = \Sigma_2$. Multiplying on the left and right by $\Sigma_1^{1/2}$ yields the equation

$$(\Sigma_1^{1/2} \Lambda \Sigma_1^{1/2})^2 = \Sigma_1^{1/2} \Sigma_2 \Sigma_1^{1/2},$$

and solving for Λ , we find

$$\Lambda = \Sigma_1^{-1/2} (\Sigma_1^{1/2} \Sigma_2 \Sigma_1^{1/2})^{1/2} \Sigma_1^{-1/2}.$$

By complementary slackness, we obtain the solution

$$\Sigma_\pi^\times = \Sigma_1 \Lambda = \Sigma_1^{1/2} (\Sigma_1^{1/2} \Sigma_2 \Sigma_1^{1/2})^{1/2} \Sigma_1^{-1/2},$$

which fully characterizes the optimal coupling π . Using the cyclic property of trace yields the Wasserstein distance

$$\begin{aligned} W_2(\mu, \nu)^2 &= \text{tr}(\Sigma_1 + \Sigma_2 - 2\Sigma_\pi^\times) \\ &= \text{tr}(\Sigma_1 + \Sigma_2 - 2\Sigma_1^{1/2} (\Sigma_1^{1/2} \Sigma_2 \Sigma_1^{1/2})^{1/2} \Sigma_1^{-1/2}) \\ &= \text{tr}(\Sigma_1 + \Sigma_2 - 2(\Sigma_1^{1/2} \Sigma_2 \Sigma_1^{1/2})^{1/2}), \end{aligned}$$

proving the theorem. □

Although the proof of [Givens and Shortt \(1984\)](#) is longer than that of [Knott and Smith \(1984\)](#), it has the advantage that it does not rely on Brenier's theorem. Therefore, we take a similar approach to [Givens and Shortt \(1984\)](#) in the proof of [Theorem 3.1](#).

D Background on the OT and GW Problems

In this section, we collect additional background on OT, GW distances, Riemannian optimization, and probability theory over Hilbert spaces.

D.1 Optimal Transport

We begin by reviewing several fundamental concepts from optimal transport; the content of this section comes mostly from Villani (2003).

The Monge-Kantorovich Problem

In 1781, Gaspard Monge formulated the problem of finding a deterministic transport map between measures. Suppose $(\mathcal{X}, d_{\mathcal{X}})$ is a Polish space (complete and separable metric space).

Definition D.1 (Monge problem). If $\mu_1, \mu_2 \in \mathcal{P}(\mathcal{X})$ and $c : \mathcal{X} \times \mathcal{X} \rightarrow \mathbb{R}$ is a cost function, the *Monge problem* is

$$\inf_{T_{\#} \mu_1 = \mu_2} \int c(x, T(x)) d\mu_1(x),$$

where the infimum is taken over all Borel-measurable functions T .

We depict the Monge problem visually in Figure 11.

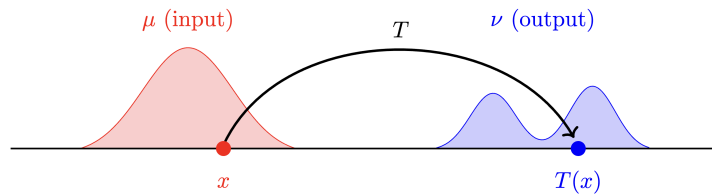


Figure 11: A visual depiction of the Monge mass transportation problem.

In 1948, Leonid Kantorovich relaxed the Monge problem to that of finding a stochastic transport plan; one motivation for the Kantorovich relaxation is that there is *no deterministic transport map* from $\mu_1 = \delta_0$ to $\mu_2 = \frac{1}{2}\delta_{-1} + \frac{1}{2}\delta_1$ and another is that the Monge problem is highly nonconvex and hard to solve in practice. Recall that $\Pi(\mu_1, \mu_2)$ denotes the set of couplings between μ_1 and μ_2 (joint distributions with marginals μ_1 and μ_2).

Definition D.2 (Kantorovich problem). If $\mu_1, \mu_2 \in \mathcal{P}(\mathcal{X})$ and $c : \mathcal{X} \times \mathcal{X} \rightarrow \mathbb{R}$ is a cost function,

the *Kantorovich problem* is

$$\inf_{\pi \in \Pi(\mu_1, \mu_2)} \int c(x, y) d\pi(x, y).$$

Equivalently, if X and Y are random variables, the Kantorovich problem is to minimize the expected cost $\mathbb{E}_\pi[c(X, Y)]$ over all joint distributions π of X and Y . Note that the Kantorovich problem is a (usually infinite-dimensional) linear program since the objective is linear in π and the constraint is convex (an intersection of linear constraints on the marginals). As long as the cost function c is lower semi-continuous (l.s.c.), it is known that the Kantorovich problem has a solution (Villani, 2003). Even though the Kantorovich problem often has a solution, it is not always unique; for example, consider the case $\mu_1 = \frac{1}{2}\delta_{(-1,0)} + \frac{1}{2}\delta_{(1,0)}$ and $\mu_2 = \frac{1}{2}\delta_{(0,-1)} + \frac{1}{2}\delta_{(0,1)}$ with the quadratic cost function.

Wasserstein Distances

We can now define the Wasserstein distances on $\mathcal{P}_p(\mathcal{X})$ as follows.

Definition D.3 (Wasserstein distances). For $p \geq 1$, the p -Wasserstein distance between measures $\mu_1, \mu_2 \in \mathcal{P}_p(\mathcal{X})$ is defined as $W_p(\mu_1, \mu_2) = \text{OT}_{c_p}(\mu_1, \mu_2)^{1/p}$, where $\text{OT}_{c_p}(\mu_1, \mu_2)$ is the optimal value of the Kantorovich problem with cost function $c_p(x, y) = d_{\mathcal{X}}(x, y)^p$.

Equivalently, the Wasserstein distance can be formulated as

$$W_p(\mu_1, \mu_2) = \inf_{\pi \in \Pi(\mu_1, \mu_2)} \|d_{\mathcal{X}}(X, Y)\|_{L^p(\pi)}.$$

The p -Wasserstein distance is a metric on $\mathcal{P}_p(\mathcal{X})$. Next, assume that c is the quadratic cost function on \mathbb{R}^d and let λ denote the Lebesgue measure on \mathbb{R}^d . An astonishing result (due to Brenier) is that as long as $\mu \ll \lambda$, the OT map is unique and is given by the graph of the gradient of a convex function. Furthermore, *any* valid transport coupling which is the gradient of a convex function is optimal.

Theorem D.1 (Brenier, 1991). *Let $\mu_1, \mu_2 \in \mathcal{P}_2(\mathbb{R}^d)$ be such that μ_1 is absolutely continuous with respect to the Lebesgue measure. Then, $\pi \in \Pi(\mu_1, \mu_2)$ is optimal for the Kantorovich problem with $c(x, y) = \|x - y\|_2^2$ if and only if there exists a proper l.s.c. convex function $\varphi : \mathbb{R}^d \rightarrow \mathbb{R}$ such that $\pi = (I, \nabla\varphi)_\# \mu_1$, where $\nabla\varphi$ is defined uniquely μ -almost everywhere.*

Using Brenier's theorem (the approach taken by Knott and Smith (1984)) or by expanding the cost directly (the approach taken by Givens and Shortt (1984)), one can compute the 2-Wasserstein

distance and OT map between Gaussian measures in closed-form; details of these two approaches and the resulting formulae are given in [Appendix C](#).

D.2 Gromov-Wasserstein Distances

In this section, we motivate and formally define GW distances ([Mémoli, 2011](#)), which provide a principled method to compare two metric measure spaces; in particular, we can use these to compare two probability distributions (possibly over different spaces) in a way that respects their underlying geometry. We begin motivating GW distances by asking the question: how can one compare two compact sets (shapes) in a metric space? One principled method is to use the Hausdorff distance (recall that $\text{dist}(a, B) := \inf_{b \in B} d_{\mathcal{X}}(a, b)$ for a compact subset $B \subseteq \mathcal{X}$ and a point $x \in \mathcal{X}$).

Definition D.4 (Hausdorff distance). The *Hausdorff distance* between compact subsets A and B of a metric space $(\mathcal{X}, d_{\mathcal{X}})$ is defined as

$$d_H(A, B) := \max \left\{ \sup_{a \in A} \text{dist}(a, B), \sup_{b \in B} \text{dist}(b, A) \right\}.$$

However, this notion of distance is overly sensitive to minor intricacies in these shapes; for instance, two shapes may be mostly identical except for a thin spike in the second one, but the Hausdorff distance will detect this and label the two sets as far apart. One way to make the Hausdorff distance less stringent, as well as to make these distances faster to compute, is to consider an L^p relaxation. In particular, we can place probability measures μ_A and μ_B over A and B respectively (which intuitively measure relative importance of features in each shape) and compute the p -Wasserstein distance between these measures. The Hausdorff distance is a metric on the set of compact subsets of a metric space $(\mathcal{X}, d_{\mathcal{X}})$. In fact, we can use the Hausdorff distance to define a notion of distance between any two compact metric spaces by minimizing over all isometric embeddings of the two spaces; this process is sometimes called *Gromovization*.

Definition D.5 (Gromov-Hausdorff (GH) distance). The *Gromov-Hausdorff* (GH) distance between two compact metric spaces $(\mathcal{X}, d_{\mathcal{X}})$ and $(\mathcal{Y}, d_{\mathcal{Y}})$ is

$$\text{GH}(\mathcal{X}, \mathcal{Y}) = \inf_{\iota_{\mathcal{X}}, \iota_{\mathcal{Y}}} d_H(\iota_{\mathcal{X}}(\mathcal{X}), \iota_{\mathcal{Y}}(\mathcal{Y})),$$

where the infimum is taken over all isometric embeddings $\iota_{\mathcal{X}} : \mathcal{X} \rightarrow \mathcal{Z}$ and $\iota_{\mathcal{Y}} : \mathcal{Y} \rightarrow \mathcal{Z}$ for some shared metric space $(\mathcal{Z}, d_{\mathcal{Z}})$.

Intuitively, the infimum is doing the work of alignment, while the Hausdorff distance measures the distance between the resulting compact sets. However, it is not clear at all how to compute the GH distance; this motivates the GW distance as an L^p relaxation of the GH distance. Of course, this means that the GW distance is a less stringent version of the GH distance. The relationships between these distances are roughly shown in Figure 12, taken from [Mémoli \(2011\)](#).

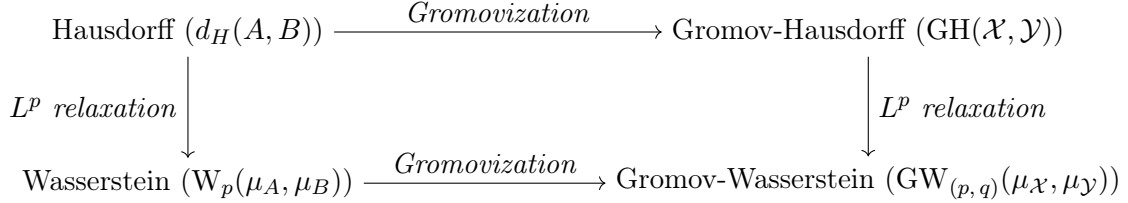


Figure 12: Relationships between various distances on spaces of objects and distributions.

We begin with a relevant definition. Recall that a *locally finite* measure space is one where every point has an open neighborhood of finite measure.

Definition D.6 (Metric measure space). A *metric measure space* (m.m. space) is a tuple (\mathcal{X}, d, μ) such that (\mathcal{X}, d) is a Polish space and $(\mathcal{X}, \mathcal{B}(\mathcal{X}), \mu)$ is a locally finite measure space.

Here are a few important examples of metric measure spaces.

Example D.1 (Euclidean space). The space $(\mathbb{R}^d, \|\cdot\|_p, \lambda)$ is an m.m. space, where $p \geq 1$ and λ denotes the Lebesgue measure on \mathbb{R}^d .

Example D.2 (Random variables). If X is an \mathbb{R}^d -valued random variable with distribution μ , then $(\mathbb{R}^d, \|\cdot\|_p, \mu)$ is an m.m. space for $p \geq 1$.

We are now ready to define the GW distance between two (not necessarily compact) m.m. spaces. Recall that $\Pi(\mu_{\mathcal{X}}, \mu_{\mathcal{Y}})$ denotes the set of couplings between $\mu_{\mathcal{X}}$ and $\mu_{\mathcal{Y}}$.

Definition D.7 (GW distance). Let $(\mathcal{X}, d_{\mathcal{X}}, \mu_{\mathcal{X}})$ and $(\mathcal{Y}, d_{\mathcal{Y}}, \mu_{\mathcal{Y}})$ be two m.m. spaces. Given $p, q \in [1, \infty)$, the (p, q) -GW distance between $\mu_{\mathcal{X}}$ and $\mu_{\mathcal{Y}}$ is defined as

$$\begin{aligned}
\text{GW}_{(p,q)}(\mu_{\mathcal{X}}, \mu_{\mathcal{Y}}) &= \inf_{\pi \in \Pi(\mu_{\mathcal{X}}, \mu_{\mathcal{Y}})} \left(\int |d_{\mathcal{X}}(x, x')^q - d_{\mathcal{Y}}(y, y')^q|^p d(\pi \otimes \pi)(x, y, x', y') \right)^{1/p} \\
&= \inf_{\pi \in \Pi(\mu_{\mathcal{X}}, \mu_{\mathcal{Y}})} \|d_{\mathcal{X}}(X, X')^q - d_{\mathcal{Y}}(Y, Y')^q\|_{L^p(\pi \otimes \pi)},
\end{aligned}$$

The (p, q) -GW distance looks for the measure coupling π between two m.m. spaces which is as close to an isometry as possible. The GW distance independently samples two pairs (X, Y) and (X', Y') according to π and minimizes the p th moment of the deviation of the q th powers of distances in \mathcal{X} and \mathcal{Y} . In this work, we analyze a variant of the GW distance, called the inner product GW distance, which was introduced in [Vayer \(2020\)](#).

Definition D.8 (IGW distance). Let $\mu, \nu \in \mathcal{P}_2(\mathcal{H})$. Then, the *inner product Gromov-Wasserstein (IGW) distance* between μ and ν is

$$\begin{aligned} \text{IGW}(\mu, \nu) &= \inf_{\pi \in \Pi(\mu, \nu)} \left(\int (\langle x, x' \rangle - \langle y, y' \rangle)^2 d(\pi \otimes \pi)(x, y, x', y') \right)^{1/2} \\ &= \inf_{\pi \in \Pi(\mu, \nu)} \|\langle X, X' \rangle - \langle Y, Y' \rangle\|_{L^2(\pi \otimes \pi)}. \end{aligned}$$

While the GW distance was looking for a measure coupling which is as close to an isometry as possible, the IGW distance looks for a measure coupling which is as close to unitary as possible. The existence of an optimal coupling for the IGW problem was shown in [Vayer \(2020\)](#). Then, IGW is a metric on the set of measures over \mathcal{H} with finite second moment, modulo unitary transformations.

Proposition D.2 ([Zhang et al. \(2025\)](#), Proposition 3.1). *The IGW distance is a metric on equivalence classes of $\mathcal{P}_2(\mathcal{H})$, where $\mu \equiv \nu$ if there exists a $(\mu \times \mu)$ -almost sure unitary transformation $\iota : \mathcal{H} \rightarrow \mathcal{H}$ with $\iota_{\#} \mu = \nu$, in the sense that $\langle x, y \rangle = \langle \iota(x), \iota(y) \rangle$ for $(\mu \times \mu)$ -almost every $x, y \in \mathcal{H}$.*

By orthogonal invariance of the IGW distance, the IGW distance can compare measures supported on different separable Hilbert spaces \mathcal{H}_1 and \mathcal{H}_2 by unitarily embedding them into a common Hilbert space ℓ^2 . Although the IGW distance looks similar in flavor to the p -Wasserstein distance, note that the objective function is no longer linear in π ; this makes the GW distance more difficult to analyze and compute in practice. However, there is a useful variational form for IGW distances in Euclidean spaces, which is discussed in [Zhang et al. \(2025\)](#). Suppose $\mu \in \mathcal{P}_4(\mathbb{R}^{d_\mu})$ and $\nu \in \mathcal{P}_4(\mathbb{R}^{d_\nu})$. Expanding the square, we find that

$$\begin{aligned} & \int (\langle x, x' \rangle - \langle y, y' \rangle)^2 d(\pi \otimes \pi)(x, y, x', y') \\ &= \underbrace{\left(\int \langle x, x' \rangle^2 d\mu(x) d\mu(x') + \int \langle y, y' \rangle^2 d\nu(y) d\nu(y') \right)}_{S_1} + \underbrace{\left(-2 \int \langle x, y \rangle \langle x', y' \rangle d\pi(x, y) d\pi(x', y') \right)}_{S_2}. \end{aligned}$$

The term S_1 has no dependence on the choice of coupling π , so it suffices to optimize over S_2 .

Proposition D.3 (Zhang et al. (2025), Lemma 2.1). *Given $A \in \mathbb{R}^{d_\mu \times d_\nu}$, define $\mathcal{T}_A(\mu, \nu)$ to be the optimal value of the Kantorovich problem between μ and ν under the cost $c_A(x, y) = -8x^\top Ay$. Then we have the following variational form, for S_2 defined as above:*

$$S_2 = \inf_{A \in \mathbb{R}^{d_\mu \times d_\nu}} \{8 \|A\|_F^2 + \mathcal{T}_A(\mu, \nu)\}.$$

Furthermore, the minimum is achieved at some

$$A \in \left[-\frac{1}{2} \sqrt{\mathbb{E}_{(X,Y) \sim \mu \times \nu} [\|X\|^2 \|Y\|^2]}, \frac{1}{2} \sqrt{\mathbb{E}_{(X,Y) \sim \mu \times \nu} [\|X\|^2 \|Y\|^2]} \right]^{d_\mu \times d_\nu}.$$

While we derive our main results about the IGW distance by expanding the square directly, note that this variational form could be used to recover some of our results in the finite-dimensional case.

E Background on Riemannian Optimization

In this section, we briefly review Riemannian gradient descent (RGD) and some properties of the Stiefel manifold. We begin by recalling several important definitions from manifold optimization theory; see Absil et al. (2008) for a more thorough treatment. Let \mathcal{M} be a Riemannian manifold and let $T_x \mathcal{M}$ denote the tangent space to \mathcal{M} at $x \in \mathcal{M}$. We let $\text{grad } f(x) \in T_x \mathcal{M}$ denote the Riemannian gradient of a function $f : \mathcal{M} \rightarrow \mathbb{R}$ at $x \in \mathcal{M}$ and let $\text{Hess } f(x) : T_x \mathcal{M} \rightarrow T_x \mathcal{M}$ denote the Riemannian Hessian of f at x .

We say that $y \in \mathcal{M}$ is a *first-order stationary point* of the optimization problem $\inf_{z \in \mathcal{M}} f(z)$ if $f \in C^1(\mathcal{M})$ and $\text{grad } f(y) = 0$. We say that $y \in \mathcal{M}$ is a *second-order stationary point* of $\inf_{z \in \mathcal{M}} f(z)$ if y is a first-order stationary point, $f \in C^2(\mathcal{M})$, and $\text{Hess } f(y) \succeq 0$.

These definitions are analogous to the standard definitions of first- and second-order stationary points in unconstrained optimization, except that the gradient and Hessian are replaced by their Riemannian counterparts. Intuitively, first-order stationary points are points where the objective function has zero directional derivative along all directions tangent to the manifold, while second-order stationary points are first-order stationary points where the objective function is locally convex along all directions tangent to the manifold.

The RGD algorithm for $\inf_{z \in \mathcal{M}} f(z)$ is analogous to the usual gradient descent algorithm, and begins with an initialization $x_0 \in \mathcal{M}$ and a step size $\alpha > 0$. Let $\text{retr}_x : T_x(\mathcal{M}) \rightarrow \mathcal{M}$ denote a retraction map onto \mathcal{M} for $x \in \mathcal{M}$. Until convergence, the RGD update is $x_{t+1} = \text{retr}_{x_t}(-\alpha \text{grad } f(x_t))$.

If it converges, RGD must converge to a first-order stationary point. Riemannian trust-region methods may be used to find second-order stationary points (as required by [Theorem 4.3](#)); see [Absil et al. \(2008\)](#) for details.

Let $\text{St}(d_1, d_2) := \{C \in \mathbb{R}^{d_1 \times d_2} : C^\top C = I\}$ denote the Stiefel manifold of orthonormal d_2 -frames in \mathbb{R}^{d_1} ; this is the manifold of interest in [Section 3](#). Recall that the Riemannian gradient of $f \in C^1(\text{St}(d_1, d_2))$ is $\text{grad } f(C) = \nabla f(C) - \frac{C}{2}(\nabla f(C)^\top C + C^\top \nabla f(C))$. Finally, we define $\text{retr}_C(G) := Q$ as the retraction onto the Stiefel manifold, where $C + G = QR$ is the QR factorization.

F Background on Random Variables in Hilbert Spaces

In this section, we collect several useful facts about Hilbert space-valued random variables. Let \mathcal{H} be a separable Hilbert space and recall ([Baker, 1973](#)) that the uncentered covariance of $\mu \in \mathcal{P}_2(\mathcal{H})$ is the bilinear form

$$\text{Cov}_\mu(x, y) := \int \langle x, z \rangle \langle y, z \rangle d\mu(z).$$

By the Riesz-Fréchet representation theorem, there exists a unique linear operator Σ such that the covariance can be written as $\text{Cov}_\mu(x, y) = \langle x, \Sigma y \rangle$; we call Σ the covariance operator of μ . The covariance operator is positive semidefinite because

$$\langle x, \Sigma x \rangle = \text{Cov}_\mu(x, x) = \int \langle x, z \rangle^2 d\mu(z) \geq 0$$

for all $x \in \mathcal{H}$ and self-adjoint by symmetry of the uncentered covariance. Fix a total orthonormal set $\{e_k\}_{k \in \mathbb{N}}$ of \mathcal{H} , so that

$$\text{tr}(\Sigma) = \sum_{k=1}^{\infty} \langle e_k, \Sigma e_k \rangle = \sum_{k=1}^{\infty} \text{Cov}_\mu(e_k, e_k) = \sum_{k=1}^{\infty} \int \langle e_k, z \rangle^2 d\mu(z).$$

Using Tonelli's theorem followed by Parseval's identity,

$$\sum_{k=1}^{\infty} \int \langle e_k, z \rangle^2 d\mu(z) = \int \sum_{k=1}^{\infty} \langle e_k, z \rangle^2 d\mu(z) = \int \|z\|^2 d\mu(z) < \infty,$$

it follows that Σ is trace-class and therefore compact. By the spectral theorem (since Σ is self-adjoint and compact), we can write $\Sigma = \sum_{k=1}^{\infty} \lambda_k(\Sigma) v_k \otimes v_k$ for nonnegative eigenvalues $\lambda_k(\Sigma) \geq 0$ and a total orthonormal set $\{v_k\}_{k \in \mathbb{N}}$ of eigenvectors. We thereby deduce

$$\text{tr}(\Sigma) = \sum_{k=1}^{\infty} \langle v_k, \Sigma v_k \rangle = \sum_{k=1}^{\infty} \lambda_k(\Sigma) \langle v_k, v_k \rangle = \sum_{k=1}^{\infty} \lambda_k(\Sigma),$$

a special case of Lidskii's trace theorem ([Simon, 2005](#)). Note that the eigenvalues cannot accumulate at a non-zero value because the covariance operators are trace-class, so it makes sense to sort the eigenvalues in descending order. Similarly, suppose we are given $\mu, \nu \in \mathcal{P}_2(\mathcal{H})$ and a coupling $\pi \in \Pi(\mu, \nu)$. Then, we can define the cross-covariance operator as the unique bounded linear operator Σ_π^\times such that

$$\text{Cov}_\pi^\times(x, y) := \int \langle x, z \rangle \langle y, w \rangle d\pi(z, w) = \langle x, \Sigma_\pi^\times y \rangle$$

for all $x, y \in \mathcal{H}$, which exists by the Riesz-Fréchet representation theorem. The cross-covariance operator is Hilbert-Schmidt because by the Cauchy-Schwarz inequality,

$$\begin{aligned} \|\Sigma_\pi^\times\|_{\text{HS}}^2 &= \sum_{k=1}^{\infty} \sum_{j=1}^{\infty} \langle e_k, \Sigma_\pi^\times e_j \rangle^2 \\ &= \sum_{k=1}^{\infty} \sum_{j=1}^{\infty} \left(\int \langle e_k, z \rangle \langle e_j, w \rangle d\pi(z, w) \right)^2 \\ &\leq \sum_{k=1}^{\infty} \sum_{j=1}^{\infty} \left(\int \langle e_k, z \rangle^2 d\mu(z) \right) \left(\int \langle e_j, w \rangle^2 d\nu(w) \right) \\ &= \text{tr}(\Sigma_\mu) \text{tr}(\Sigma_\nu) \\ &< \infty. \end{aligned}$$

Finally, given any $m \in \mathcal{H}$ and trace-class self-adjoint positive semidefinite operator Σ , there exists a unique Gaussian measure $\mathcal{N}(m, \Sigma) \in \mathcal{P}_2(\mathcal{H})$ with mean m and covariance operator Σ ; see [Bogachev \(1998\)](#) for details. This measure is characterized precisely by the property that for any $h \in \mathcal{H}$, the pushforward measure $(h \otimes h)_\# \mathcal{N}(m, \Sigma)$ is a univariate Gaussian with mean $\langle h, m \rangle$ and variance $\langle h, \Sigma h \rangle$.